COMBINE GRAIN LOSS TRANSDUCER DESIGN

by

JAMES DOMENIC SCHARPLAZ

B. S., Kansas State University, 1973

A MASTER'S THESIS

submitted in partial fulfillment of the

requirements for the degree

MASTER OF SCIENCE

Department of Agricultural Engineering

KANSAS STATE UNIVERSITY

Manhattan, Kansas

1975

Approved by:

Stanley J. Clark

Major Professor

Combine Grain Loss Transducer Design

(James D. Scharplaz, B.S. 1973)

TABLE OF CONTENTS

LIST OF FIGURES

LIST OF FIGURES (continued)

LIST OF FIGURES (continued)

LIST OF FIGURES (continued)

INTRODUCTION

The grain combine is one of the most complicated machines used in agriculture, yet it operates without the benefit of an effective feedback control system that could make it much more efficient. This is because it is very difficult to equip a combine with the transducers required to measure the performance of the machine and feed it back to a controller. Whether the controller is electronic or a human operator, it cannot function without information about the operation of the machine.

Only a few parts of the combine are equipped to monitor their operation. The engine has gauges and a tachometer which gives some information about load. The machine may be equipped with a cylinder tachometer, fan tachometer, and a ground speed indicator. Some warning systems may be installed to warn of plugged elevators or straw plugging the straw walkers, and some parts of the machine, such as the reel and header, are visible to the operator. Furthermore, an experienced operator can gain information about his machine from what he hears and the vibrations he feels.

Still, a great deal of information is not available, chiefly in the area of grain quality and losses. Some progress has been made in the area of monitoring walker and chaffer losses, but there is presently no way to measure unthreshed grain loss, and the operator seldom even considers broken kernels.

The purpose of this research was to find a way to monitor unthreshed grain loss. This problem is a difficult one because the unthreshed heads are so hard to detect in the cloud of straw blowing out of the machine. Many schemes to sample the straw for unthreshed heads were considered, but, due to the immensity of this task, none of them showed much promise. Besides the sheer volume of material to be caught and handled, there was the problem of rethreshing and separating it. Of course, all this had to be done without disturbing the operation of the combine.

Zaidi's work (Zaidi, 1974), provided the key to the problem, pointing out an indirect method of predicting unthreshed grain loss. He found a correlation between the ratio of the amount of grain threshed at the front of the concave to the amount of grain threshed at the rear of the concave and the number of unthreshed heads. Zaidi's work was done on a small laboratory cylinder equipped with a sectioned concave, pans to catch the grain threshed on the various sections, and a box to catch the straw. After a test run, he counted the contents of the various pans and related that information to the number of unthreshed kernels he found in the box.

The problem of measuring unthreshed grain loss reduced to developing a transducer that could collect the same information from a combine operating in the field that Zaidi found by counting the seeds in his pans. The transducer would be used to confirm Zaidi's results under field conditions by installing it on machines equipped to catch their straw for cleaning and rethreshing. If his findings held true, the transducer could then be used as a guide to adjust the machine to reduce unthreshed grain loss.

The chief problem in designing the transducer is that there was no way to check its operation on the machine, except by whether or not it eventually gave information that correlated with the amount of unthreshed grain. If it did not there would still be a question as to whether the transducer was faulty, or whether Zaidi's findings did not apply to field conditions. Therefore, every effort was expended to make sure the transducer would work as intended. This is the reason for the complicated process required to design

REVIEW OF LITERATURE

The desirability of controlling various parts of the combine automatically have been evident for some time. Friesen, et al (1966), experimented with automatic feed rate control. Their device sensed cylinder load by measuring the tension in the cylinder drive chain, and adjusted ground speed to keep the feed rate constant. The system was totally mechanical, employing an idler wheel that moved as chain tension increased, actuating a hydraulic valve through a system of levers. The hydraulic valve controlled a cylinder which adjusted the variable speed ground drive sheave. The tension in the drive chain was counterbalanced by a spring; a viscous damper eliminated load peaks. For equal average feed rates, the automatically controlled machine lost less grain than standard combines. According to the author, this was due to the fact that losses increase exponentially with feed rate. The automatic machine was slower in dense crop areas and faster in light crop areas than standard machines.

Another popular subject of automation attempts has been header height control. Especially in down crops or in crops such as soybeans, running the header as close to the ground as possible results in increased yield, as well as increased danger of damage to the header. Automatic control of header height offers more precise control and decreased danger of header damage.

Bredfeldt (1968) designed a hydraulic system to automatically control header height. Height sensing fingers or shoes maintained contact with the ground at all times. If the header moved too close to the ground, the height sensors forced the pin of an adjustable metering valve into its seat, which raised system pressure. This caused the platform to rise until the pressure returned to equilibrium. The setpoint could be easily adjusted from the operator's position. Manual control could be resumed by pulling the header height control valve from the automatic control detent position. The system successfully controlled header height between two and six inches off the ground, but it wasted power and became hot when the header was lifted to its full height. This was due to the design of the hydraulic system.

A different approach to header height control was taken by Story, et al (1968). He reasoned that in standing grain, there was an optimum header height--low enough to cut most of the grain, yet high enough to avoid cutting excess straw, which increases losses. To measure the height of the heads of the crop, the degree of attenuation of a beam of microwaves was measured. Since the kernels attenuated the waves much more than the straw, the device could be used to find the position of the heads of the crop, and position the header accordingly. The system had the advantage that it was not as susceptible to weed patches and bare spots as mechanical crop height sensors. It was not reduced to practice and tested in the field.

Kaminski and Zoerb (1963) developed a mechanical header height control system. It employed two microswitches actuated by lever arms, mounted one above the other. When the bottom switch was closed and the top switch was open the header was at the proper height. When both switches were closed, the header was too low, and when both switches were open, the header was too high. The switches activated electrically controlled hydraulic valves which moved the header up and down. This system could not measure the position of the lower heads, and was susceptible to irregularities due to the small area the levers sampled.

Acoustic Loss Monitors

One device which actually measures losses, rather than loss producing conditions, such as cylinder overload, is the acoustic grain loss monitor. Reed, et al (1969), report the development of such a device. Soundings boards were mounted beneath the ends of the straw walkers, and under the end of the cleaning shoe. Extensions and chutes on the ends of the walkers deflected the kernels and chaff passing the ends of the walkers onto the sounding boards, where the impact of the kernels produced vibrations which were picked up by a transducer. The signals were filtered to remove low frequency components. All the signals below a certain level were removed by a discriminator, and the pulses were squared up by a monostable signal conditioner. Finally, a frequency to voltage converter changed the pulses to an analog voltage indicative of bushels per hour.

In laboratory tests, the system could detect eighty-six percent of the kernels falling randomly, with a maximum rate of two hundred impacts per second for evenly spaced impacts. Satisfactory output resulted from kernels falling from a minimum of four inches to a maximum of nine feet. The circuits were stable from minus twenty degrees Fahrenheit to one hundred thirty-five degrees Fahrenheit.

The device was tested in the field with a batch collector that caught all the material leaving the walkers and cleaning shoe. The material was cleaned to retrieve the loose kernels and the average rate of loss was calculated. The results indicated that the device was a practical combine attachment. Loss could be detected the moment it started and the rate of loss could be determined. As the rate of loss increased, the proportion of loss detected by the monitor decreased. The author hypothesized that this was due to grain being carried out of the machine in the straw mat.

Proportionally fewer kernels of barley were counted as compared to wheat. This was assumed to be due to the awns still attached to some barley kernels, preventing adequate impact. Various resistors were provided to make the dial read bushels per hour for different types of grain.

Zaidi's Research

The work of Zaidi (1974) is of major interest in this design. He did research attempting to define criteria for threshability of various varieties of wheat. He used a laboratory cylinder instrumented to measure torque, and equipped with a concave divided into six sections from front to back (hereafter termed positions one through six). Pans under the respective concave sections were provided to catch the grain that was threshed on each section. He ran many bundles of different varieties of wheat through the cylinder in a statistically designed series of tests. He reported a correlation between the percentage of kernels found in the section nearest the front of the concave (first position) and the amount of unthreshed grain that left the cylinder. Since that percentage was dependent on the feedrate, he also correlated the amount of unthreshed grain to the ratio of the amount at the first position and another concave position. Again a correlation was found, although not quite as significant as for the percentage relationship. The correlation was strongest for the ratio of first to sixth and first to fifth sections.

There is some question, of course, as to whether the relationship holds true for field machines, since the laboratory cylinder was fed bundles rather than a continuous flow of grain. There were also many other differences in size and conditions between the laboratory cylinder and a field machine.

INVESTIGATION

The objective of this research was to develop a transducer capable of measuring the amount of grain threshed at a particular point on a combine concave. The intention was not to accurately measure the total amount of grain threshed for a concave area, but to produce a value proportional to this amount. The ratio of the values produced by two of these transducers would give information for a field combine similar to the information Zaidi (1974) got for his laboratory cylinder. If Zaidi's laboratory work is valid for field conditions, two transducers should provide information for grain loss monitoring and/or feedback signals for travel speed, cylinder speed, or concave clearance control.

Preliminary Considerations

The primary concern, of course, was to produce a device capable of measuring cylinder loss. No possibility was rejected without consideration. Before Zaidi's work was finished, various methods of measuring cylinder loss directly (by catching samples of straw and determining the number of unthreshed heads) were discussed. Zaidi's results terminated this discussion, for two reasons. First, it appeared to be a much simpler system. The process of catching and finding the unthreshed heads in the volume of straw required for a representative sample required machinery too large and complex to be considered a simple monitor. The chances of such a system producing continuous cylinder loss data were very low. Second, monitoring the cylinder loss at the cylinder had advantages from a control standpoint. Loss would be monitored as it occurred, not several seconds later. This would give earlier warning of loss, and thus a more efficient monitoring system. Also, the reduction in time lag would enable a control system to react faster with less overshoot and less danger of instability. This would make the monitor much more useful if it were used as part of the control system of an automated combine.

There are two ways to consider the kernels coming through the concave for measurement purposes. They can be measured as a rate of mass flow: either continuously, like an in-line scale does, or in increments, like a tipping balance; or as individual kernels, by counting. The counting method was chosen because it permitted the use of a transducer that could function inside the combine. It also presented the further advantage of being directly usable in a digital control system. Considering the complexity of fully automating a combine, and the recent advances in digital electronics, the chances are very good that a control system for a fully automated combine will be a digital system.

Attempt at a Mass Flow Monitor

A monitor to be used under the concave of a combine must endure a noisy and dirty environment. It is subject to damage and obstruction from dust and straw, and it must reject sound and mechanical vibration, as well as be insensitive to gross movements of the machine. The first attempt to design a monitor fell victim to the environment problem.

The first monitor worked on the mass flow principle. The intention was to build a small chute that would catch grain from an area of the concave about two by six inches and direct it across a pan mounted on a cantilever beam. The beam would deflect proportionally to the amount of grain on the pan, and strain gauges would measure the deflection. The purpose of the chute was to remove the effect of the velocity of the kernels as they entered the device.

To design the beam, an estimate was needed of the amount of grain that could be expected to flow through the two-by-six-inch chute. Assuming a combine with a twenty-foot header operating at four miles per hour in forty-bushel-per-acre wheat, the machine would thresh three hundred-eighty-seven pounds of grain per minute. According to Kepner, et al (1972), combines with twenty-foot headers have cylinders averaging forty-six inches wide. The average concave area of the two largest machines of six manufacturers, all with concaves in the forty-six-inch range, is nine hundred five square inches (Implement and Tractor, 1974). This means that an average of .43 pounds of grain would pass through each square inch of concave per minute. Observation of kernel counts done by Zaidi (1974) indicate that about twice as much grain is threshed at the front as at the back of the concave. Therefore, the cantilever beam should be designed to give maximum deflection while weighing .86 pounds of grain per minute per square inch of area sampled. For the two-by-six-inch sample area this is 10.32 pounds per minute.

For a particular flow rate, the number of kernels that would be present on the scale pan at a given time depends on the velocity of the kernels as they move down the chute. To get an idea of the amount of wheat that would be on the monitor's scale pan at different flow rates, a test chute was constructed. The chute was two inches wide and inclined at thirty degrees. It was equipped with two gates that could be snapped shut to trap the wheat on a two-by-two-inch area of the chute. This chute was tested using flow rates up to sixteen pounds per minute. The results of the tests are shown in Figure 1.

The information in Figure 1 was used to calculate the size of beam required to deflect sufficiently to produce a usable output with a certain load.

THIS BOOK CONTAINS NUMEROUS PAGES WITH DIAGRAMS THAT ARE CROOKED COMPARED TO THE REST OF THE INFORMATION ON THE PAGE.

THIS IS AS RECEIVED FROM CUSTOMER.

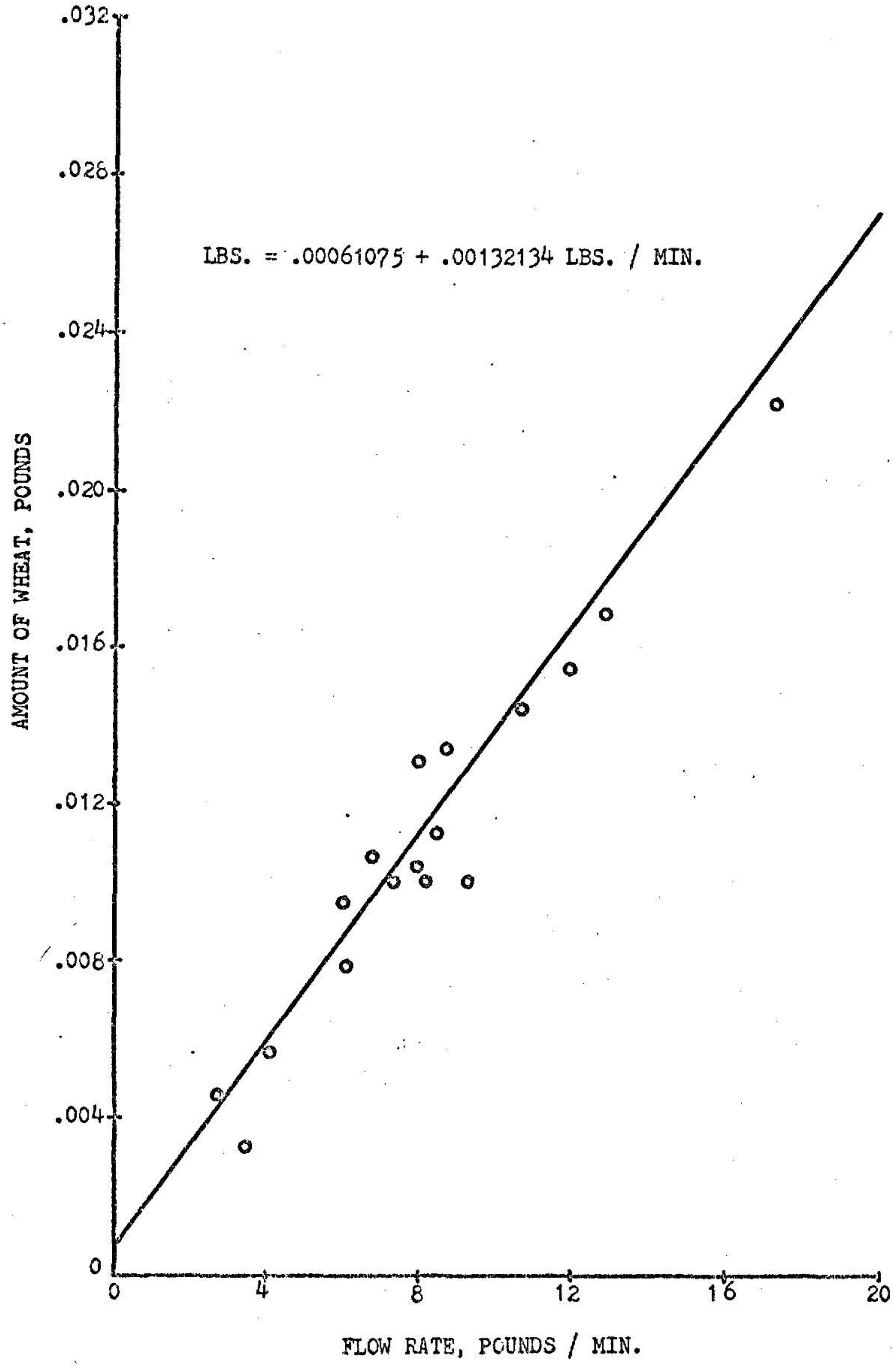

Figure 1. Amount of wheat found on a 2" x 2" area of a chute for various flow rates.

Appendix A shows a sample calculation using the load for 10.32 pounds per minute, .0142 pounds, and lists several other design restrictions. The natural frequency of the beam-pan combination used in the calculations was 1.624 radians per second, which corresponds to fifteen revolutions per minute. This frequency is well within the range of vibrational frequencies that could be expected from a combine. Frequencies for other loads are shown in Figure 2. Even if the load values in Figure 1 were far in error, the natural frequency of the resulting beam would still lie well within the range of vibrational frequencies of a combine. Therefore, the device would become excited, and there would be a large noise signal present in the output of the device. For this reason, and because the device seemed susceptible to plugging with straw and chaff, the design of a cantilever beam type weighing device was terminated.

Designing a Counting Type Monitor

After brief consideration of other mass flow schemes, such as microwave and capacitance devices (rejected due to complexity), attention centered on a counting method of measuring the flow of kernels. The only useful property of a kernel of grain to detect its presence as it passes through a combine concave is its kinetic energy. With all the straw and chaff that is present, it is impossible to detect it optically. Its resistance is so high that it cannot be detected as it bridges two conductors, and the size of one kernel is insignificant compared to the area of an air dielectric capacitor of sufficient size to function below the microwave range.

However, the kinetic energy of a kernel as it strikes a diaphragm produces an impulse that can be counted. The mass of the kernel is so much greater than any other particle in the stream of grain and chaff that there is no problem differentiating them.

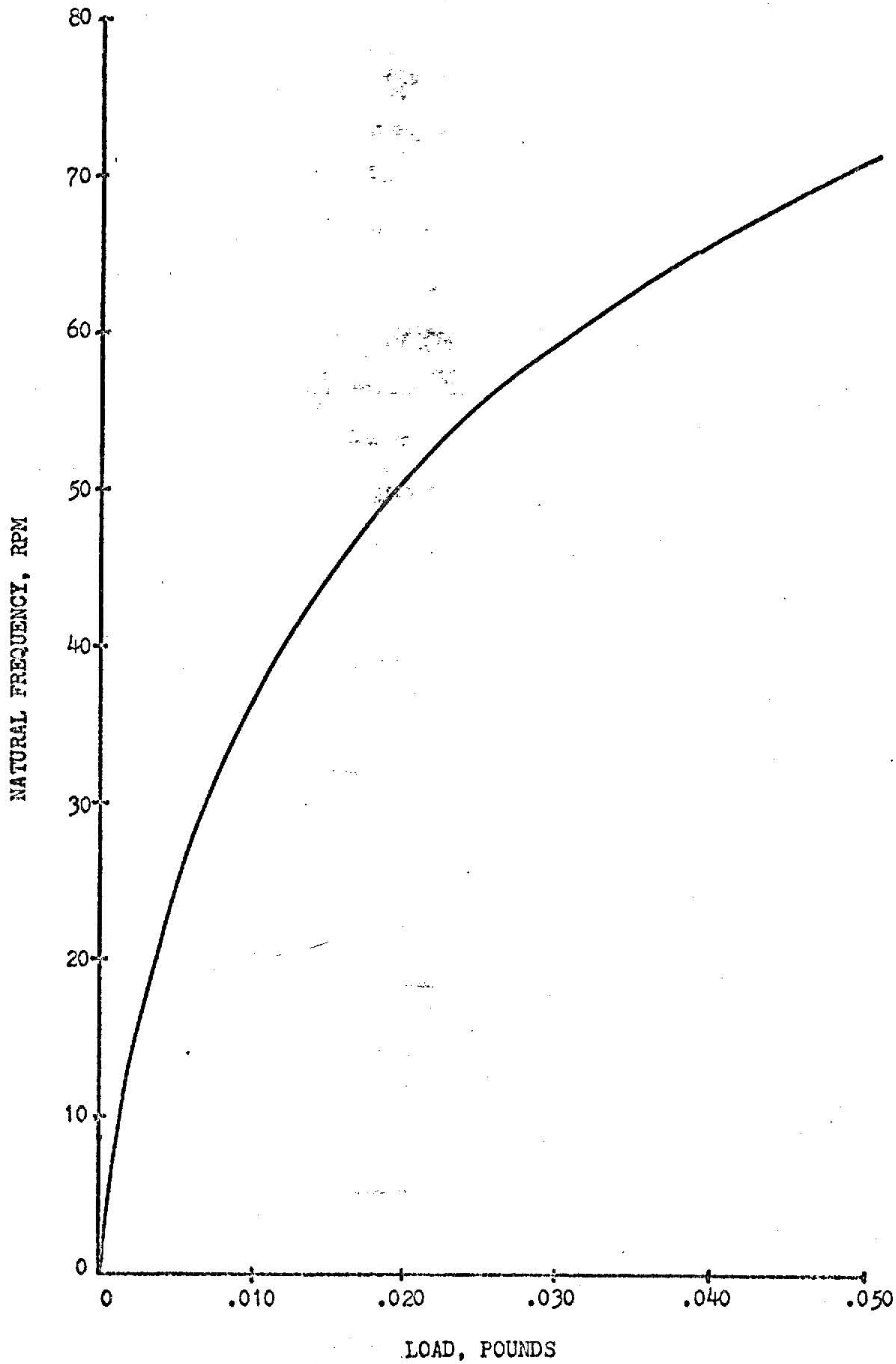

Figure 2. Natural frequency of cantelever beams designed to produce

An impact-type kernel counter consists of two active parts. They are the diaphragm which the kernels strike, and the transducer which converts the motion of the diaphragm into an electrical signal. These two parts are held together by a body or frame. See Figure 3.

The chief consideration in the design of a counting-type monitor is the maximum attainable counting rate. The counting rate is controlled by the length of the pulse that is counted. The pulse length is determined by the length of time the kernel stays in contact with the diaphragm, and the length of time the diaphragm oscillates after the kernel leaves its surface. In the case of every diaphragm tested in this study, the oscillations were the only significant part of the pulse length. This conclusion is drawn on the basis that the waveform changed chiefly in amplitude, slightly in duration, and retained the same shape no matter what struck the diaphragm.

The diaphragm was chosen on the basis of three things: pulse length, pulse height, and how much the signals decreased in height as the impacts moved from the center to the edge of the diaphragm.

The test counter diaphragms were round, one inch in diameter. See Figure 4. This size was chosen because it would not significantly affect the operation of the combine, and because the number of kernels striking a one-inch diameter counter represented a count rate that we felt we could achieve. For the same conditions as were used for the cantilever beam device, a maximum rate of .68 pounds per minute should strike the transducer. If there are thirteen thousand wheat kernels in a pound (Brumfield, 1970), the required count rate is 8780 seeds per minute, or 146 seeds per second.

If the kernels were to strike the counter at evenly spaced intervals, a 6.8 millisecond pulse length would be acceptable. However, the incidence of the kernels on the diaphragm is random. Therefore, there is a chance that

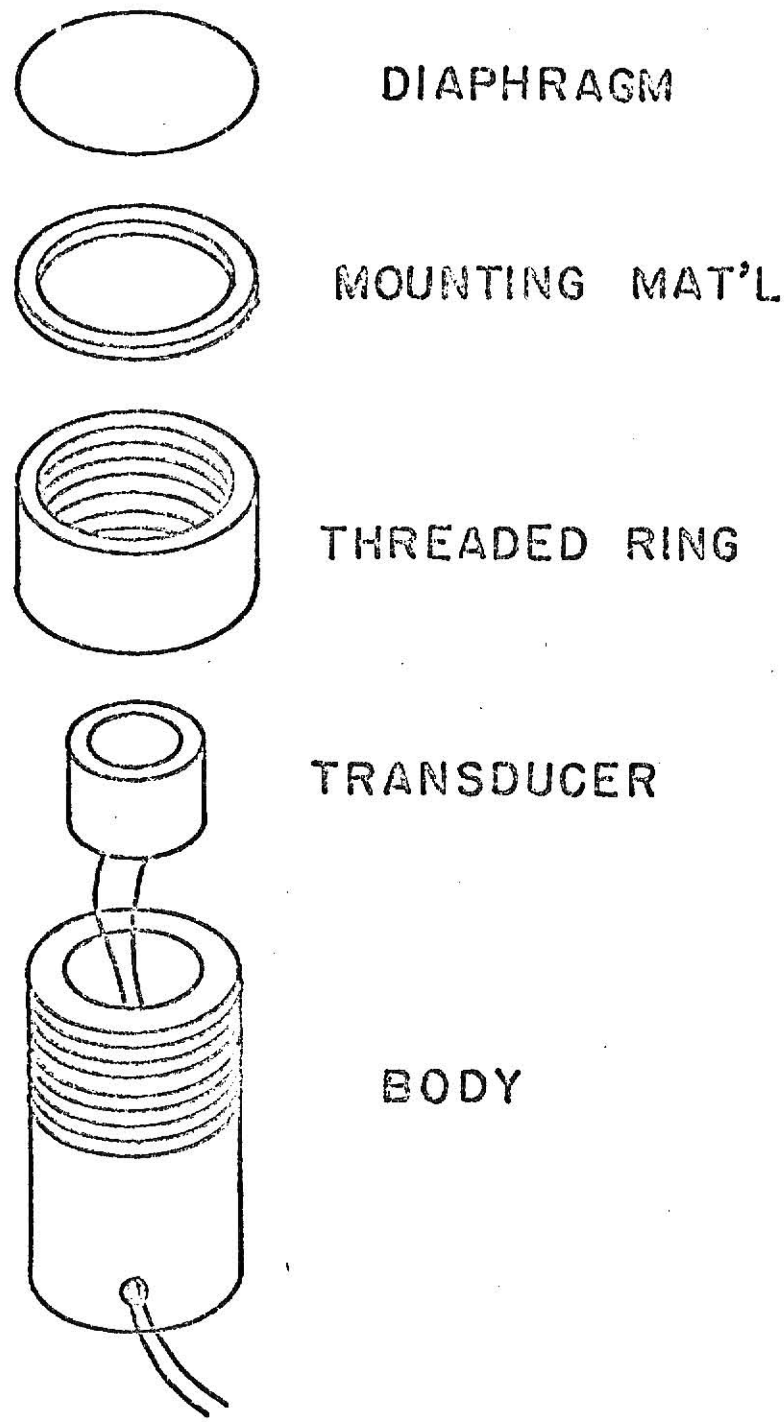

Figure 3. Assembly view of counter.

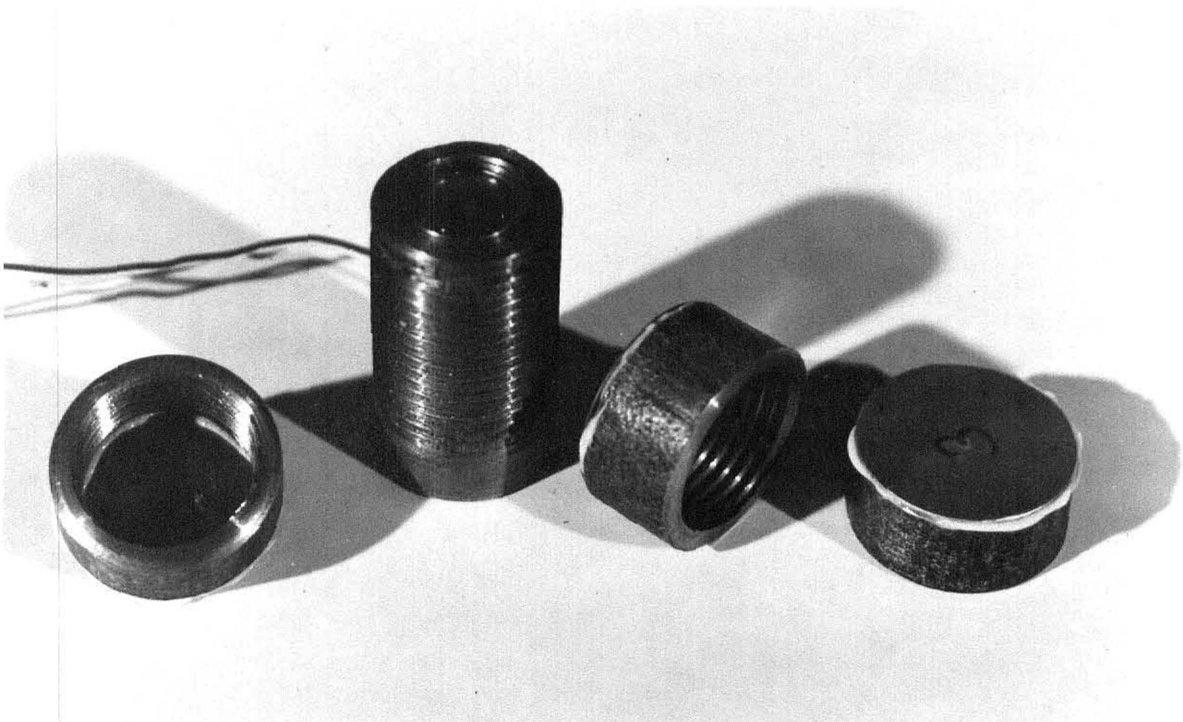

Figure 4. Disassembled counter and three diaphragms.

two kernels will strike during the same time period and be counted as one. The probability of this occurring is a function of the pulse length and the rate of flow. Figure 5 shows the probability of two kernels striking the counter within a particular time period for different flow rates. See Appendix B for the derivation of this figure. Since the distribution is random, the possibility of error exists no matter how low the count rate is.

Individual Impact Testing

The selection of the best diaphragm proceeded in two main steps. First, the best diaphragm material was selected by observing the waveforms produced by the impact of individual objects. The best diaphragm was defined as the one producing the shortest pulse length, greatest amplitude, and least attenuation of signal as a function of distance from the center of the diaphragm.

The counter was fastened to a ring stand with a clamp and inclined fifteen degrees from the vertical to prevent bouncing. Number six lead shot were dropped four inches onto the diaphragm and the resulting pulses were stored and observed on a Tektronic Type 564 Storage Oscilloscope equipped with a Type 3A74 Four Trace Amplifier and a Type 2B67 Time Base. Shot were used to insure uniformity, and they were guided by a trough and tube arrangement to make sure each one hit the same spot. See Figure 6 for details.

Copper, steel, aluminum, and polyethylene diaphragms were tested. All were .020 inches thick and one inch in diameter. Five of each kind were mounted elastically, with silicone sealer, and five more of each kind were mounted inelastically with epoxy. To make the diaphragms easily interchangeable, they were fastened to threaded rings which were screwed onto the body of the counter; see Figure 3. Ten shot were dropped at each of four positions

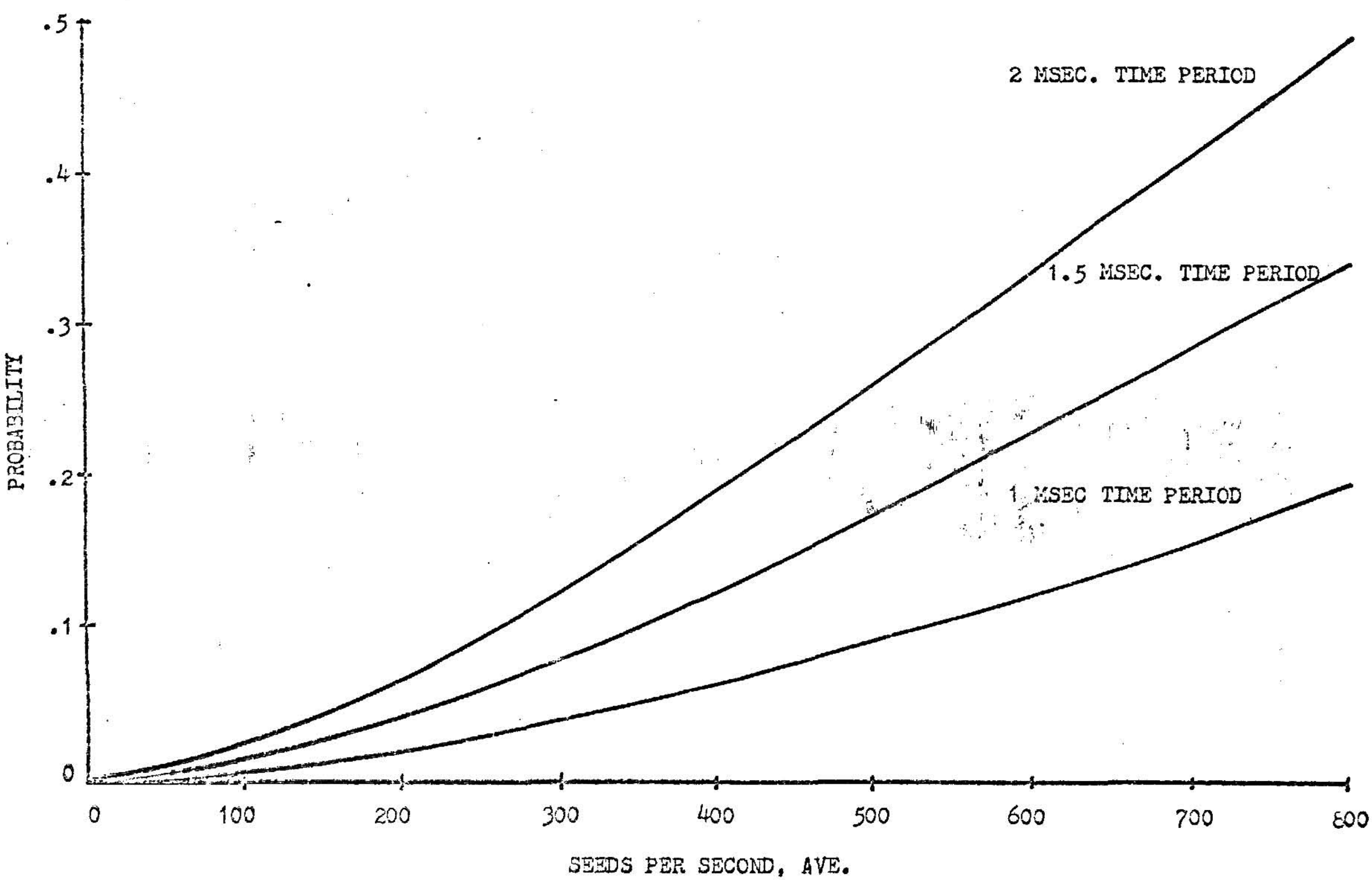

Figure 5. Probability of two seeds falling in the same time period.

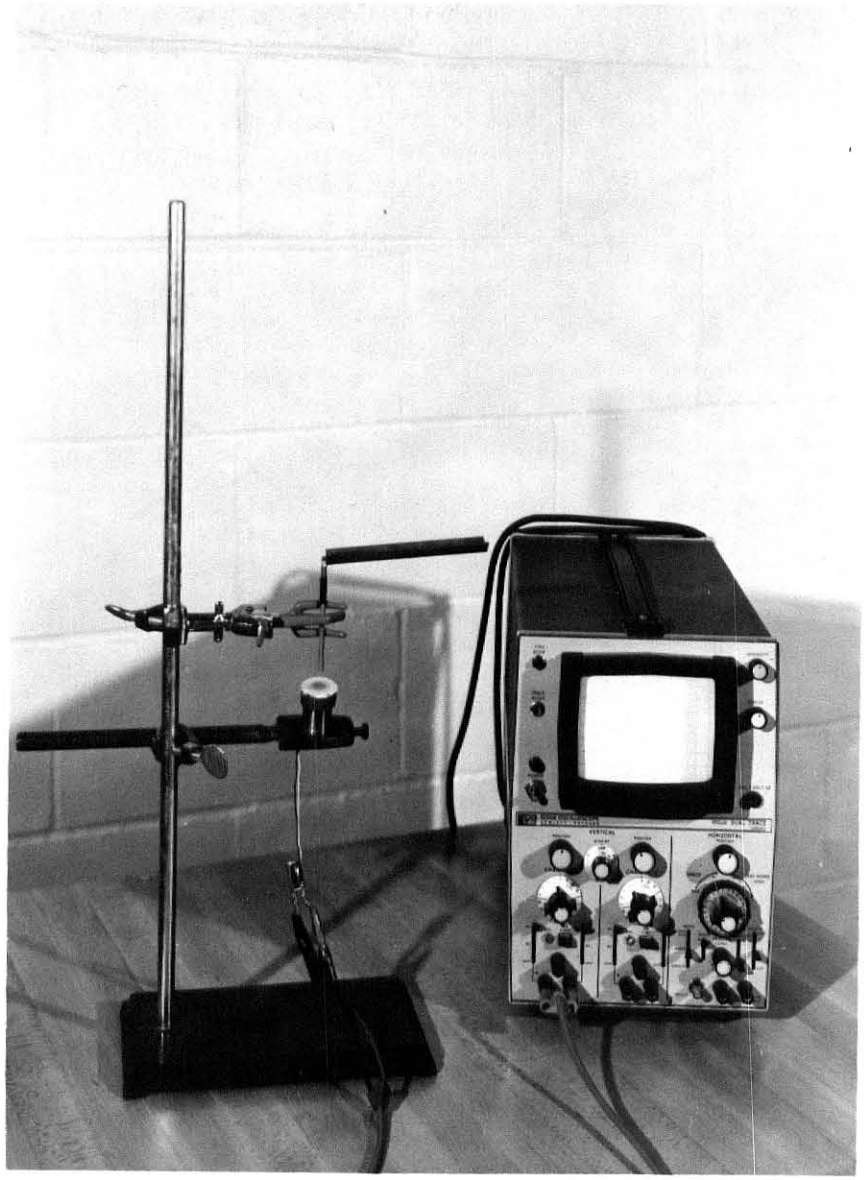

Figure 6. Experimental set-up for tests with lead shot.

on each test diaphragm. The four positions were the center, .16 inches from the center, .32 inches from the ceter, and the edge of the diaphragm. A total of sixteen hundred shot were dropped. Each pulse was individually observed, and its maximum height and its length were recorded. The pulse length was determined by the length of time required for the signal to fall below a certain level, which varied depending on the average maximum amplitude for that diaphragm and waveform, but was usually one fifth of the maximum voltage.

The following pages contain a series of oscilloscope photographs, taken on a Tektronic Type 503 Oscilloscope using a Tektronic Type C-27 Camera System and Polaroid Type 107 film. The waveforms shown were chosen as typical of the test conditions they represent. Appendix C contains the raw data taken, and pertinent means. The oscilloscope was adjusted for the largest possible trace for each group of five diaphragms.

Figures 7, 8, 9 and 10 show the difference between elastic and inelastic mounting. Not only did the elastic mount produce greater amplitude, but the signal decayed faster, which would permit a shorter pulse length and faster counting.

Figures 11, 12, 13, and 14 illustrate the differences between the four diaphragm materials that were tested. These characteristic waveforms held for all positions and particles, except for changes in amplitude. Notice that the polyethylene diaphragm not only produced a larger signal with a shorter pulse length, but produced a lower frequency signal. The lower frequency is advantageous because it is easier to define the pulse length of the low frequency signals, and because transducers with poorer frequency response (therefor cheaper) can follow the lower frequency signals. The frequency of the diaphragm is roughly inversely proportional to the modulus of elasticity of

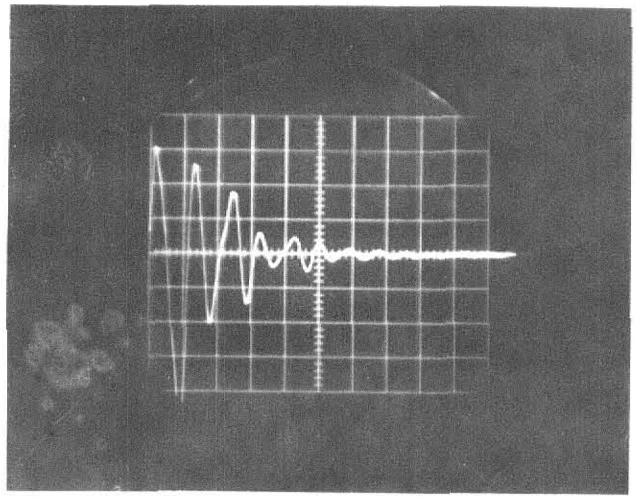

Figure 7. Trace produced by the impact of a lead shot on an inelastically mounted polyethylene diaphragm. 1 volt/div., .5 msec./div.

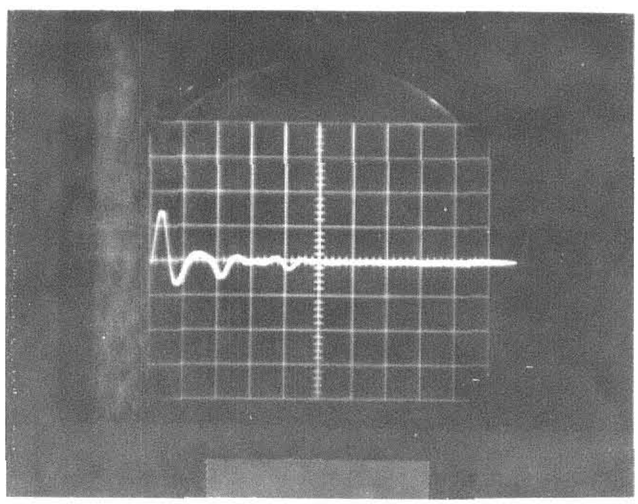

Figure 8. Trace produced by the impact of a lead shot on an elastically mounted polethylene diaphragm. 5 volts/div., .5 msec./div.

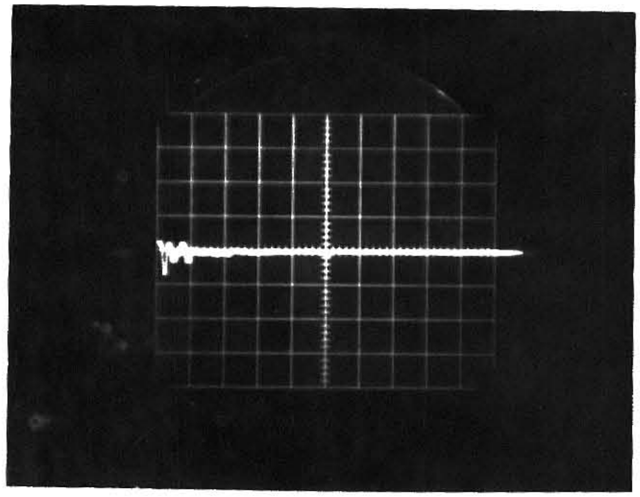

Figure 9. Trace produced by the impact of a kernel of wheat on an inelastically mounted polyethylene diaphragm. .5 volts/div., 1 msec./div.

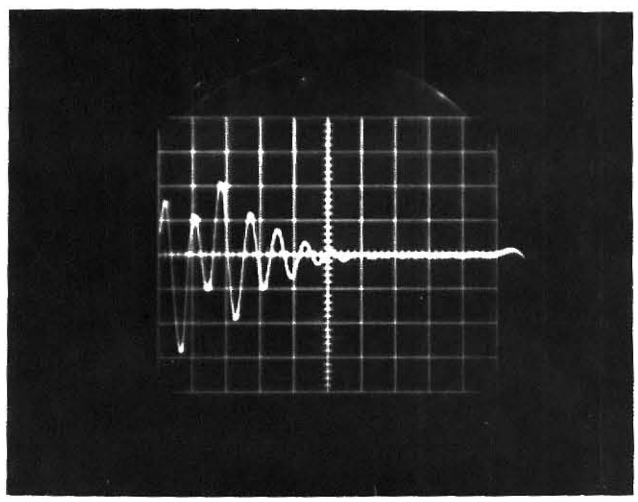

Figure 10. Trace produced by the impact of a wheat kernel on an elastically mounted polyethylene diaphragm. .5 volts/div., .5 msec./div.

the diaphragm material (Table 1), which is as it should be since the spring constant depends on the modulus of elasticity. Notice from Figures 11 and 12 or 13 and 14 that the mounting material doesn't seem to have any effect on the frequency of the signal.

Table 1. Modulus of Elasticity and Diaphragm Frequency for the Various Diaphragm Materials.

Material	Modulus of * Elasticity (psi, Pa)	Frequency ** (cps)
Steel	30×10^6, 2.07×10^{11}	5000
Copper	17×10^6, 1.17×10^{11}	4000
Aluminum	10×10^6, 6.89×10^9	3500
Polyethylene	$.10 \times 10^6$, 6.89×10^8	2500

* Bolz and Tuve, 1970
** Determined by observation of oscilloscope traces.

Figures 14, 15, 16, and 17 illustrate how the signal amplitude decreases with distance from the center of the diaphragm. This decrease was present in all of the materials but was not nearly as predictable for some of them, since the signals became very small and erratic toward the edge. Figure 18 shows a signal from an object that struck the diaphragm over the threaded ring. Its amplitude is roughly .1 that of a signal from just inside the ring. This indicates that the part of the diaphragm over the ring should not be considered part of the effective area of the diaphragm. A similar indication of the degree of attenuation for wheat can be gained by comparing Figure 19 to Figure 10.

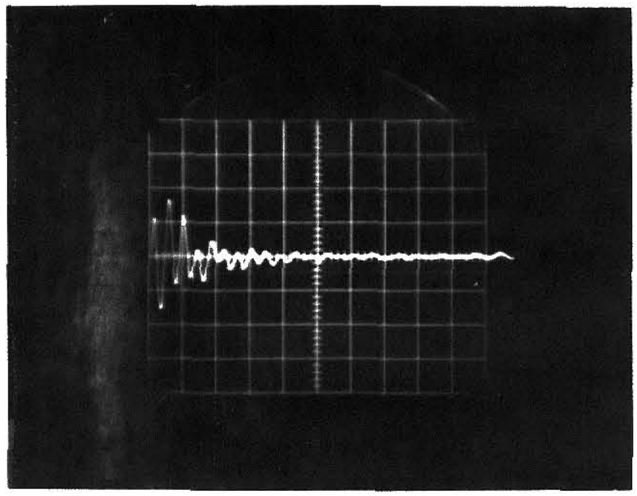

Figure 11. Trace produced by the impact of a lead shot on an elastically mounted steel diaphragm. .5 volts/div., .5 msec./div.

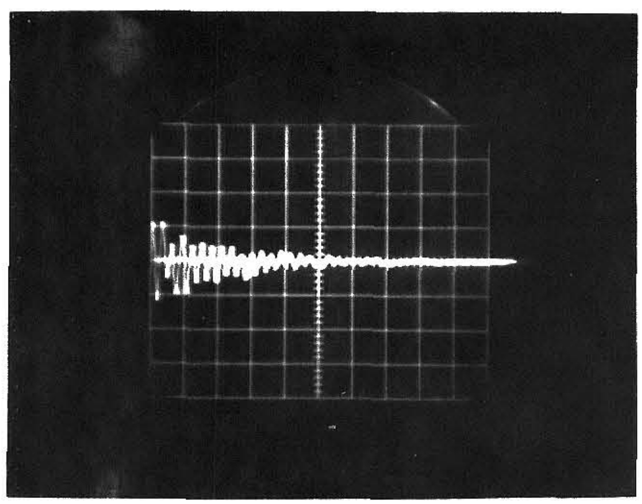

Figure 12. Trace produced by the impact of a lead shot on an elastically mounted copper diaphragm. .5 volts/div., 1 msec./div.

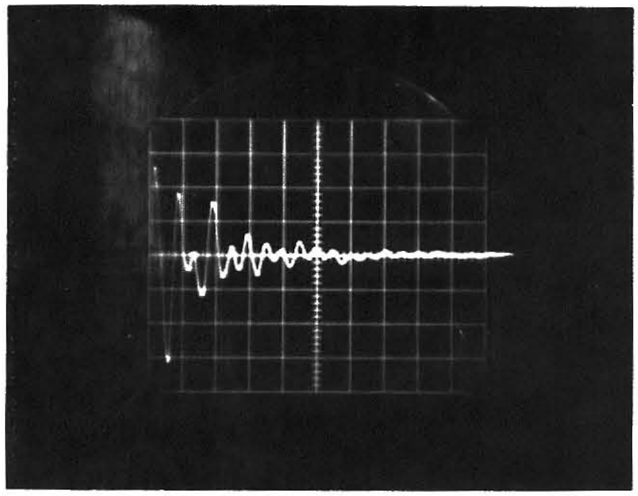

Figure 13. Trace produced by the impact of a lead shot on an elastically mounted aluminum diaphragm. 1 volt/div., .5 msec./div.

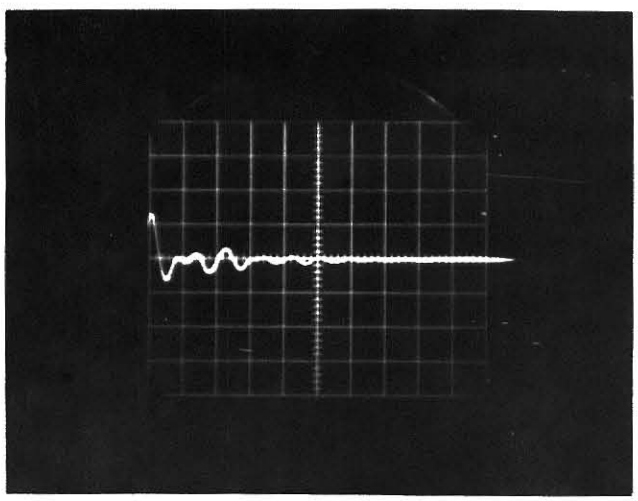

Figure 14. Trace produced by the impact of a lead shot at the center of an elastically mounted polyethylene diaphragm. 5 volts/div., .5 msec./div.

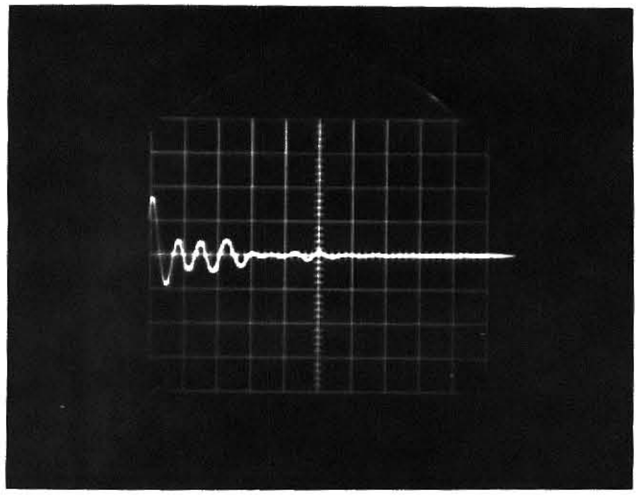

Figure 15. Trace produced by the impact of a lead shot .16 inch from the center of an elastically mounted polyethylene diaphragm. 5 volts/div., .5 msec./div.

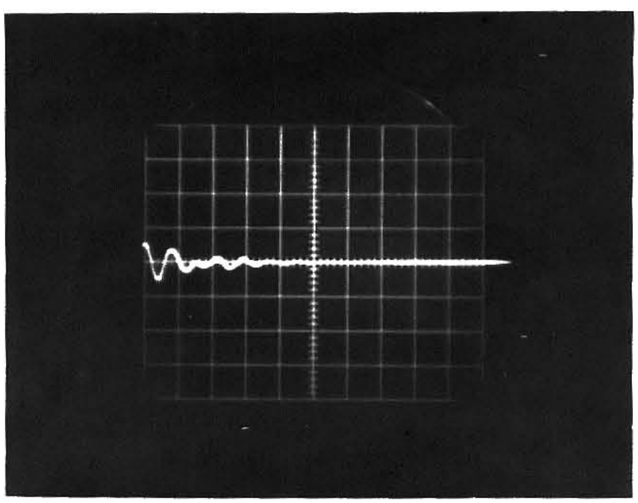

Figure 16. Trace produced by the impact of a lead shot .32 inches from the center of an elastically mounted polyethylene diaphragm. 5 volts/div., .5 msec./div.

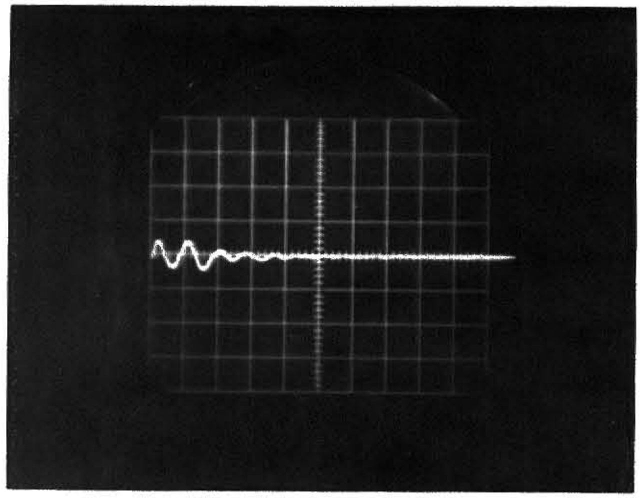

Figure 17. Trace produced by the impact of a lead shot at the edge of an elastically mounted polyethylene diaphragm. 5 volts/div., .5 msec./div.

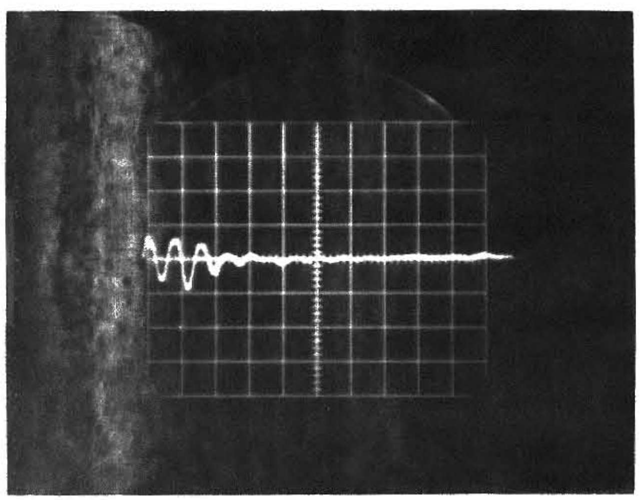

Figure 18. Trace produced by the impact of a lead shot over the mounting ring of an elastically mounted polyethylene diaphragm. .5 volt/div., .5 msec./div.

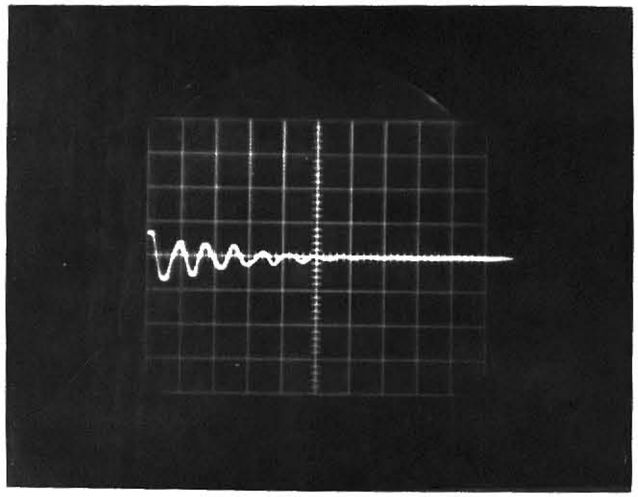

Figure 19. Trace produced by the impact of a wheat kernel at the edge of an elastically mounted polyethylene diaphragm. .5 volts/div., .5 msec./div.

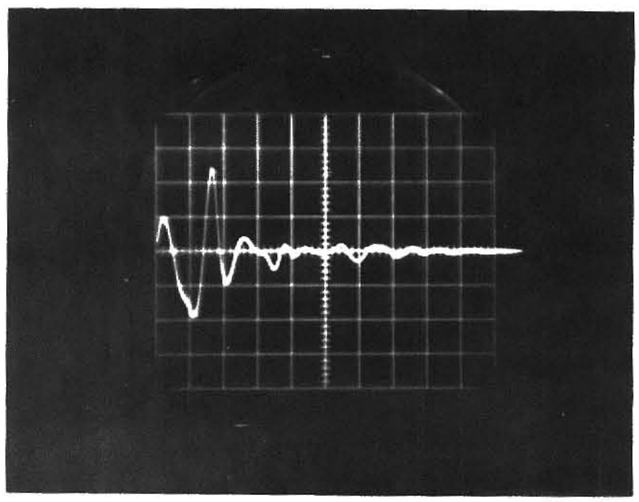

Figure 20. Trace produced by the impact of a corn kernel on the center of an elastically mounted polyethylene diaphragm. 5 volts/div., .5 msec./div.

As a matter of interest, the counter was also tested with corn and milo. Except for differences in amplitude and some slight changes in waveform, the output signal was very much the same, Figures 20 and 21.

Figure 22 illustrates a phenomenon the experimenter referred to as a double bounce. The exact cause of this is not known, but it was hypothesized that it was caused by the wheat kernel landing on its end, then falling over on its side to produce another pulse. Lead shot, milo, and other round objects never produced a signal such as this, which tends to support the theory. When the same object produced two pulses by striking, bouncing up and striking again, the pulses were at least five milliseconds apart because the oscilloscope always triggered twice.

Reed, et al (1969), felt that barley sometimes failed to trigger their acoustic counter if it still had awns attached. This experimenter noted a similar phenomenon in that wheat kernels landing hair end down seemed to produce a smaller signal than those oriented the other way. This is only a general observation and is not supported by data, since there is no way to be sure that wheat kernels dropped hair end down actually landed that way.

On the basis of observations of traces such as these, and on the basis of the data in Appendix C, elastically mounted polyethylene diaphragms were determined to perform best.

Flow Rate Testing

Having selected the diaphragm, further tests were made on the performance of the counter as a whole. A vibratory feeder and a funnel (Figure 23) were used to direct various flow rates of wheat onto the counter, which was equipped with an elastically mounted polyethylene diaphragm. The pulses were counted by a Hewlett Packard 5212A Electronic Counter. The flow was counted

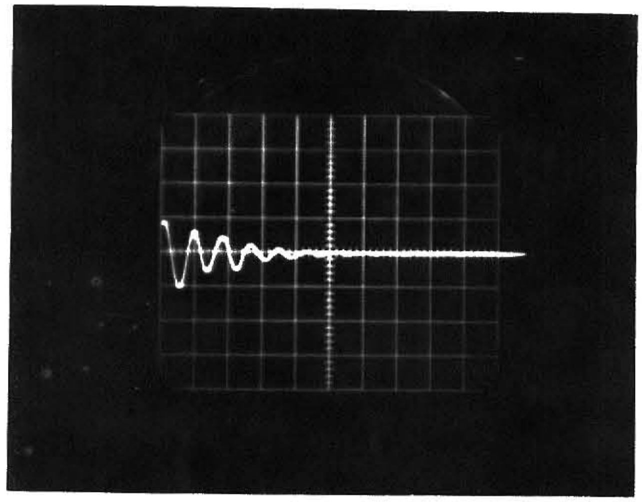

Figure 21. Trace produced by the impact of a milo kernel on the center of an elastically mounted polyethylene diaphragm. 1 volt/div., .5 msec./div.

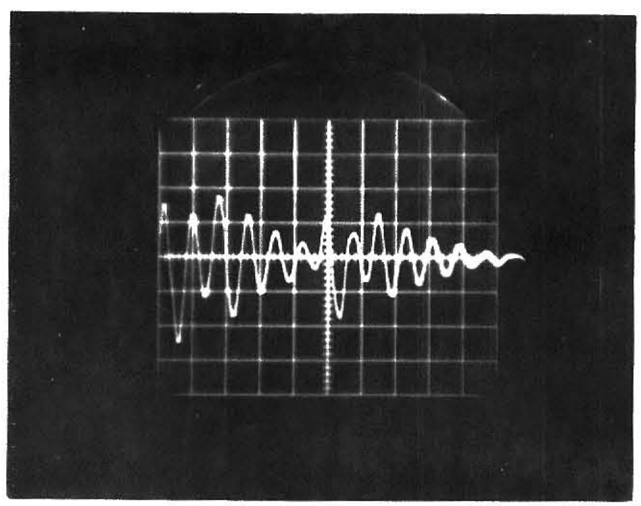

Figure 22. Double bounce trace produced by the impact of a wheat kernel on an elastically mounted polyethylene diaphragm. .5 volt/div., .5 msec./div.

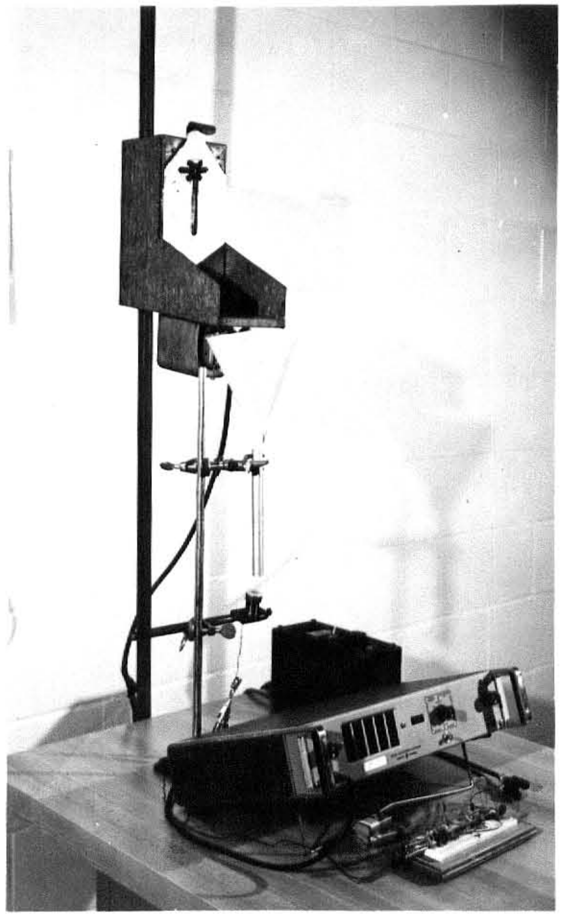

Figure 23. Experimental set-up for flow rate tests with wheat. Second funnel which caught seeds after counting has been removed to show counter.

for one minute, one-half minute, or one-quarter minute, depending on the rate. The kernels were caught as they bounced off the counter and were recounted with an Audiotronics Electronic Seed Counter to determine the actual flow rate. The data are in Appendix D and are graphed in Figures 24, 25, and 26. The counter was tested using pulse lengths of 1.0, 1.5, and 2.0 milliseconds and flow rates to nearly sixty-five thousand seeds per minute. The term pulse length refers to the pulse length of a monostable multivibrator in the counting circuitry. Once this monostable multivibrator was triggered, another seed could not be counted until the pulse was over.

The curves of the test counts were fitted by a version of the Doolittle statistical analysis program. A weighted, constrained, polynomial regression analysis was performed, resulting in the equations in Table 2. The curves were constrained to pass through the origin, and the coefficient of the linear term was set at .81403. To determine this value, the ratio of the experimental counts to actual counts was taken. This ratio remains constant up to a certain number of counts and then begins to drop off. The average of all the ratios of all the counts up to the drop off point is .81403. The analysis was weighted by assuming that if the variance of a one-minute sample period was one, the variance of a one-half minute sample period would be two, and the variance of a one-quarter minute sample period would be four.

The resulting overall estimate of standard deviation was 328.15. It was not recommended that these equations be used to predict counts beyond 50,000 seeds per minute.

The discrepancy between the actual performance of the counter and perfect operation, which would be represented by a line with a slope of one in Figures 24, 25, and 26, could be due to any or all of several factors. First, some seeds are missed due to double strikes. Figures 24, 25, and 26 show

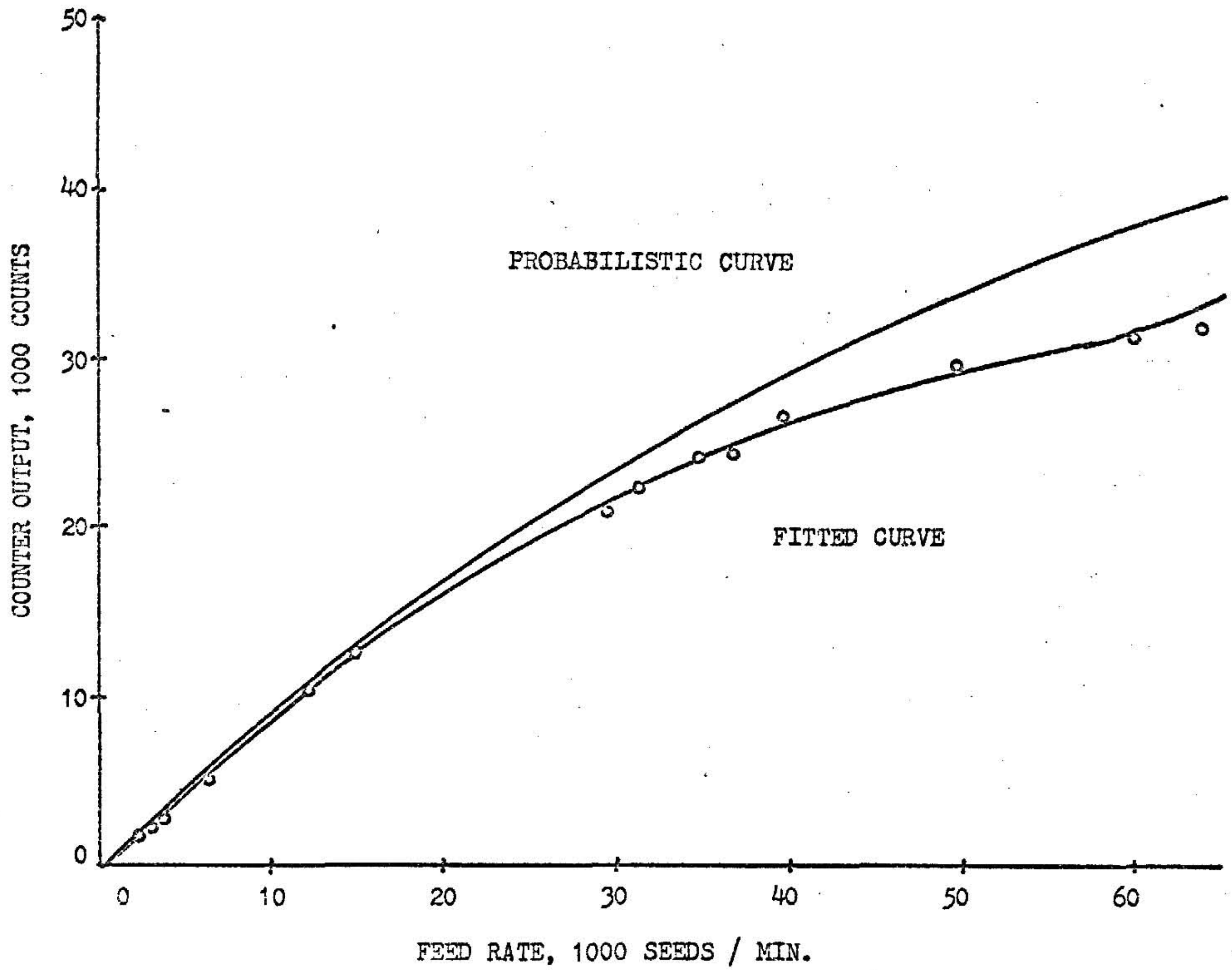

Figure 24. Counter output at various feed rates with 1 msec. pulse length.

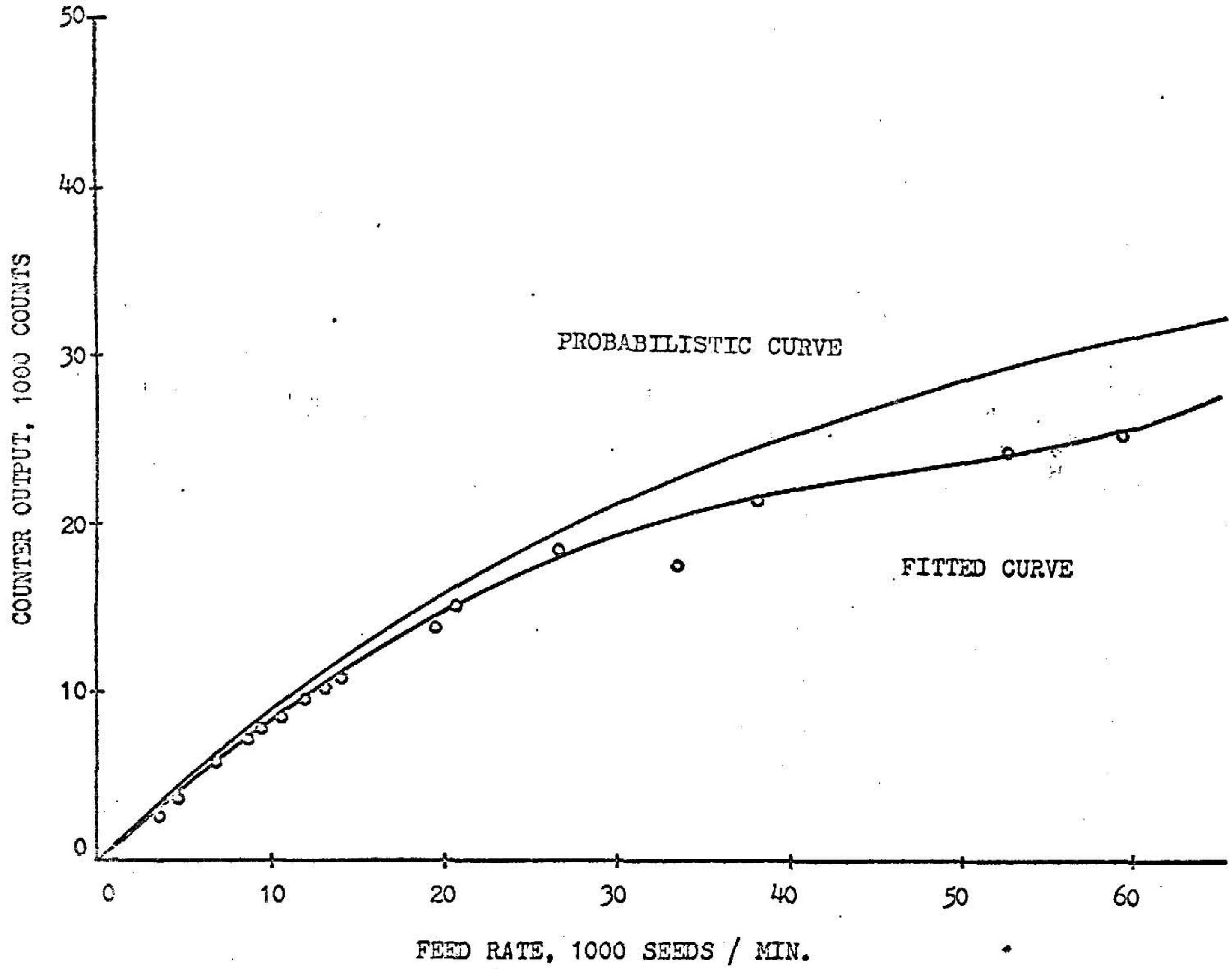

Figure 25. Counter output at various feed rates with 1.5 msec. pulse length.

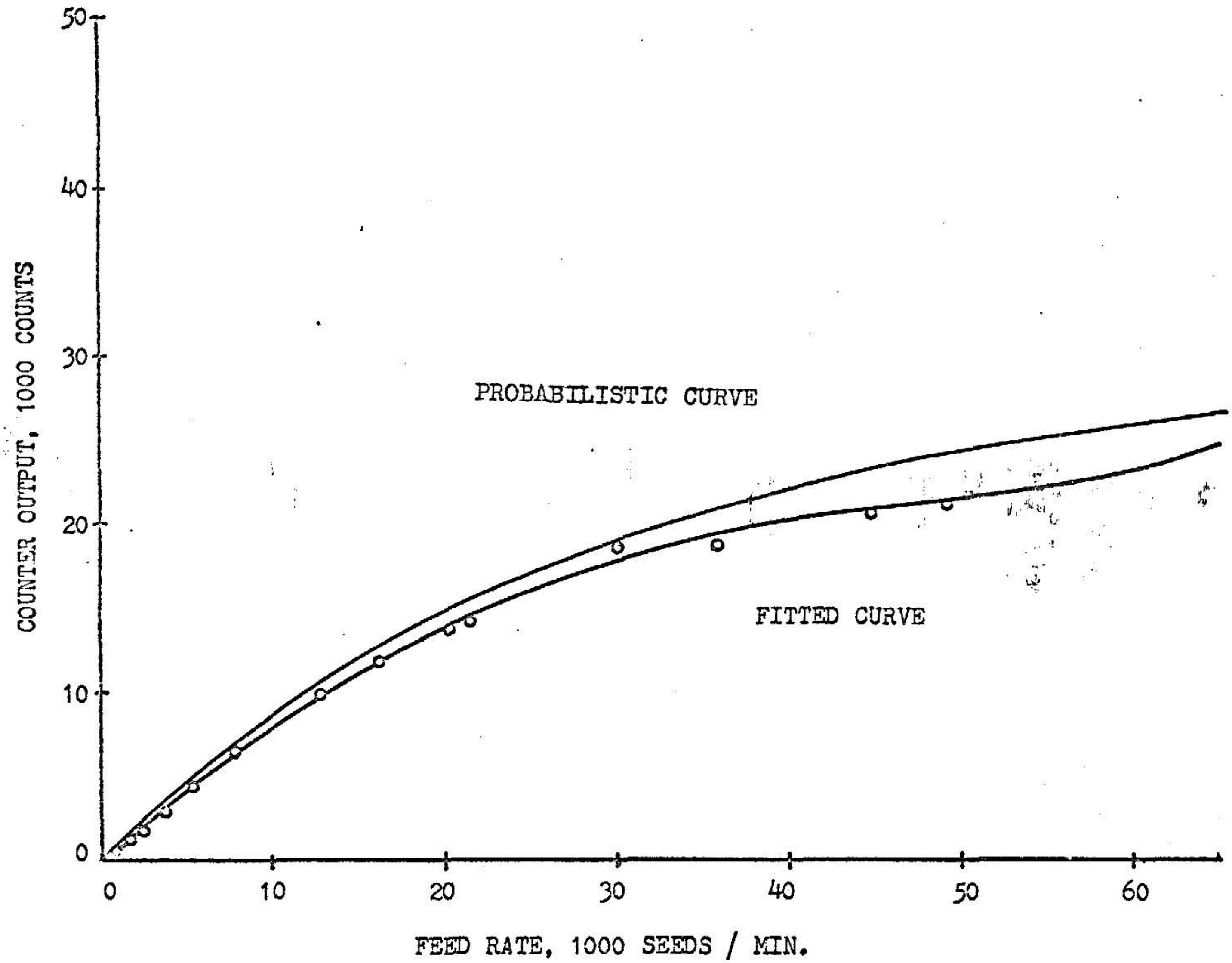

Figure 26. Counter output at various feed rates with 2 msec. pulse length.

Table 2. Fitted Equations for Transducer Output as a Function of Flow Rate.

General Equation	$\hat{y} = \beta_0 + \beta_1 x + \beta_2 x^2 + \beta_3 x^3 + \beta_4 x^4$
Pulse Length (msec.)	Coefficient
2.0	$\beta_0 = 0$ $\beta_1 = .81403$ $\beta_2 = -2.5496402 \times 10^{-6}$ $\beta_3 = -2.3625701 \times 10^{-10}$ $\beta_4 = 2.6626254 \times 10^{-15}$
1.5	$\beta_0 = 0$ $\beta_1 = .81403$ $\beta_2 = -5.4256660 \times 10^{-8}$ $\beta_3 = -2.8234013 \times 10^{-10}$ $\beta_4 = 2.9376865 \times 10^{-15}$
1.0	$\beta_0 = 0$ $\beta_1 = .81403$ $\beta_2 = 4.3107971 \times 10^{-6}$ $\beta_3 = -3.2278807 \times 10^{-10}$ $\beta_4 = 2.8683336 \times 10^{-15}$

curves of predicted performance that take double strikes into account. These curves show the probability of at least one strike in a time period equal to one pulse length. They were developed in the same manner as the curves in Figure 5, which show the probability of an error--two or more strikes in one pulse length. The procedure is explained in Appendix B. It is not entirely valid to predict performance in this manner, because it assumes the pulses counted are very short compared to the time period. That is, if a second kernel falls during a time period, probabilistically it is lost. Actually, if it falls near enough the end of the period, the signal it produces will extend out of the period and be counted. At any rate, it can be seen that this theory alone does not explain the error accurately enough to match the actual count curves. Second, an especially heavy seed may produce a pulse long enough to be counted twice. Third, perfect performance is established by the Audiotronics optical counter. This counter counts shriveled and broken kernels and pieces of dust that the impact counter cannot detect. Finally, there is a possibility that the seeds were physically interfering with each other at some of the higher flow rates.

The Transducer

It may have been noted that relatively little emphasis has been placed on the transducer part of the counter. This is true for two reasons. First, the experimenter had no control over the design of the transducer, simply using microphone elements purchased locally. Second, the transducer was not a critical part of the design. Any number of transducers with response far greater than necessary are available. The only consideration is that the transducer be immune to vibration. For this reason, a high quality crystal element is recommended, with response to around ten thousand hertz. Capacitance and resistance elements would also work, but are not preferred since they are more complicated and require a power supply. For the experimental work a Realistic MC-1000 element was used. It had excellent response, but was sensitive to vibration, being of the dynamic type. Figure 27 illustrates the result of using an element with too low response, an inexpensive crystal model with response to about two thousand hertz. The crystal itself has been excited and is oscillating rather than tracking the oscillations of the diaphragm. Compare this picture with Figure 7.

Signal Processing

The output of the transducer is not compatible with electronic counters. The several peaks of each signal would produce multiple counts, and it was necessary to provide the counter with pulses of uniform amplitude and to eliminate noise signals. It seemed that a circuit to make the signal compatible was a logical final step, so a circuit was designed to produce one uniform wave form for each variable pulse.

The circuit had to do three things. It was to differentiate between signals and noise, prevent multiple triggering, and produce a countable waveform. The classical method of dealing with this problem, which is widely used in debouncing switches, for example, is to use a monostable multivibrator. The monostable multivibrator triggers when the signal rises above a certain level, and stays on, regardless of what the signal does, for a length of time longer than the signal lasts.

The circuit is block diagrammed in Figure 28. It has three main parts, the first two of which are detailed in Melem and Garland (1971). Figure 29 shows the schematic diagram of the circuit. The first part is made up of resistors R_2 and R_3 which serve as a level detector that separates the signal

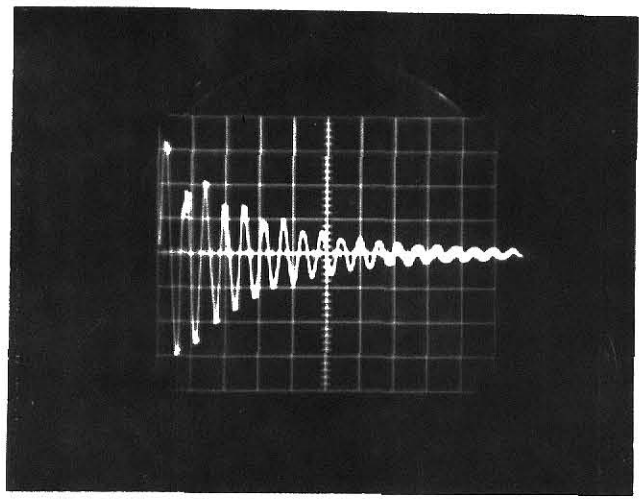

Figure 27. Trace produced by the impact of a lead shot on an elastically mounted polyethylene diaphragm with a slow transducer. 2 volts/div., 1 msec./div.

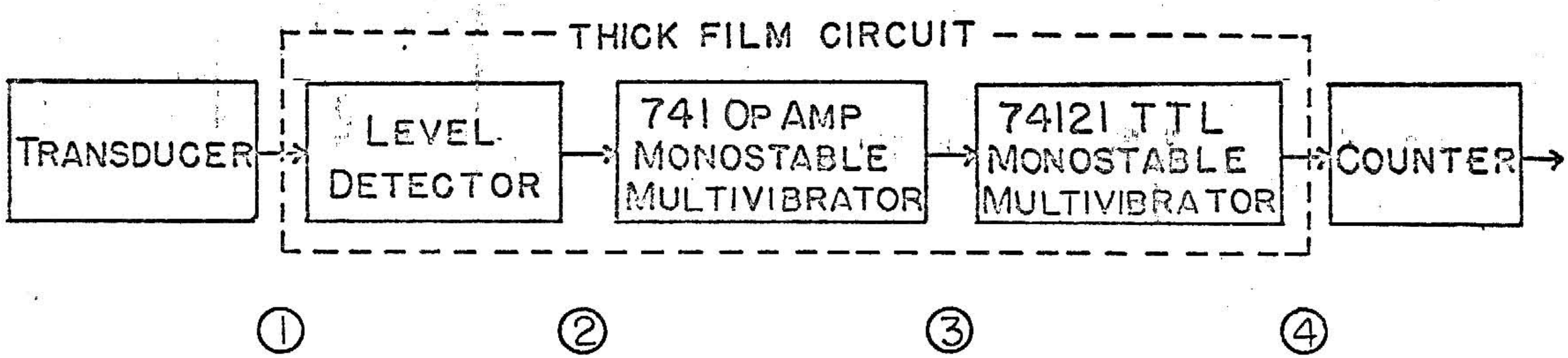

Figure 28. Block diagram of the signal processing circuit. The signal at points 1 through 4 is shown in Figures 30 through 33.

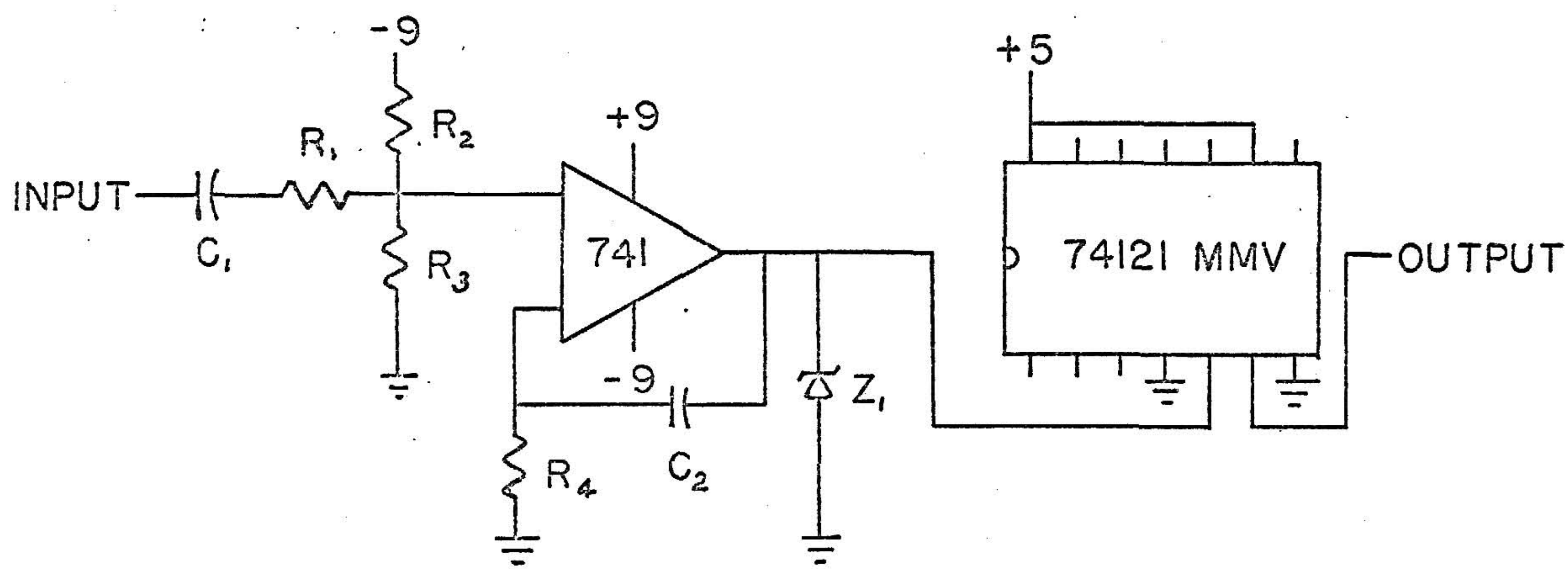

$R_1, R_3 = 5{,}000\ \Omega$ $\qquad$ $C_1, C_2 = 8200$ pF $\qquad$ $Z_1 = 4$ Volt

$R_2 = 445{,}000\ \Omega$

$R_4 = 26{,}000\ \Omega$

Figure 29. Schematic diagram of the signal processing circuit.

from low level noise. They produce a negative voltage at the input of the first monostable multivibrator. To trigger the monostable multivibrator, the signal must be large enough to produce a net positive voltage at the input (Figure 31). Figure 30 is included for comparison. The second part is a monostable multivibrator made up of a 741 operational amplifier and its associated components C_2, R_4, and Z_1. R_4 and C_2 determine the length of time the monostable pulse lasts, and Z_1 limits its output voltage to make it compatible with the next stage. When no signal is being received, the first monostable multivibrator produces four volts D.C. When a signal arrives, its output drops to zero volts for the set time, and then returns to four volts. See Figure 32. This monostable output pulse is what hides the various peaks of the input signal and determines the maximum counting rate of the counter. The third stage is a 74121 TTL monostable multivibrator. It is connected in a standard manner suggested by the manufacturer to produce a thirty nanosecond pulse every time the first monostable multivibrator returns to four volts. See Figure 33. The short output pulse means that the output of several transducers can be added together with little chance they will overlap, losing a count. Also the output of this monostable multivibrator is compatible with TTL counters. Since TTL is generally the most restrictive of the various logic families, a system that is TTL compatible is usually compatible with other logic systems, or can easily be made compatible.

The circuit was produced in thick film (Figure 34). This allowed it to be reduced to a two-inch by three-quarter-inch chip. Thick film technology has several advantages for agricultural applications. The primary one is that it is the most economical production system to use when producing the number of circuits that would be required for agricultural applications. It is much smaller than printed circuits, yet it is more flexible than monolithic con-

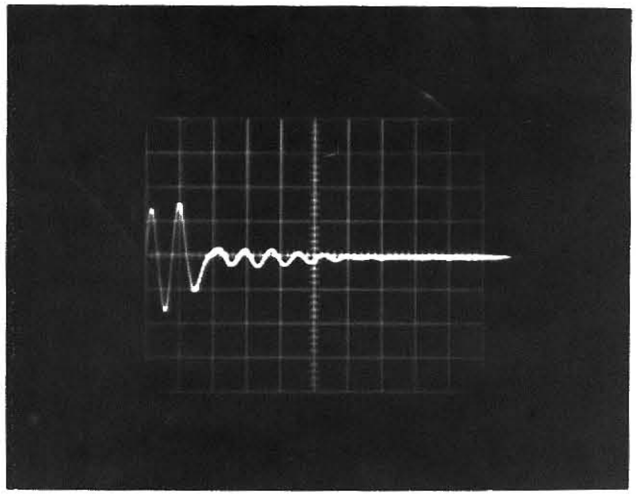

Figure 30. Input to signal processor. Wheat kernel on elastically mounted polyethylene diaphragm. 1 volt/div., .5 msec./div.

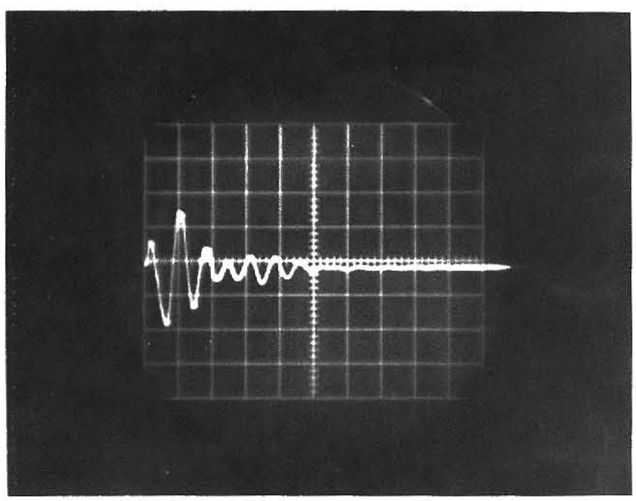

Figure 31. Input signal after comparator stage. Wheat kernel on elastically mounted polyethylene diaphragm. 1 volt/div., .5 msec./div.

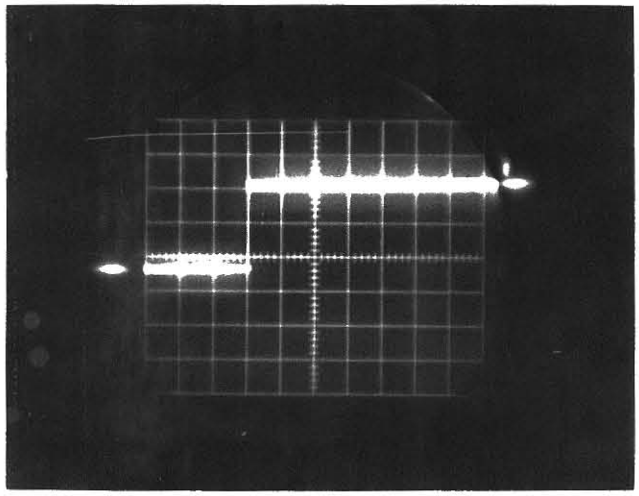

Figure 32. Output of the first monostable multivibrator stage.
2 volts/div., .5 msec./div.

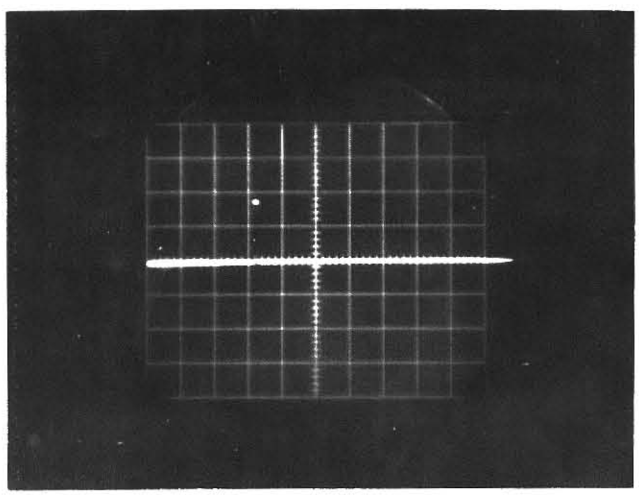

Figure 33. Output of the final monostable multivibrator stage, lengthened for visibility. 2 volts/div., .5 msec./div.

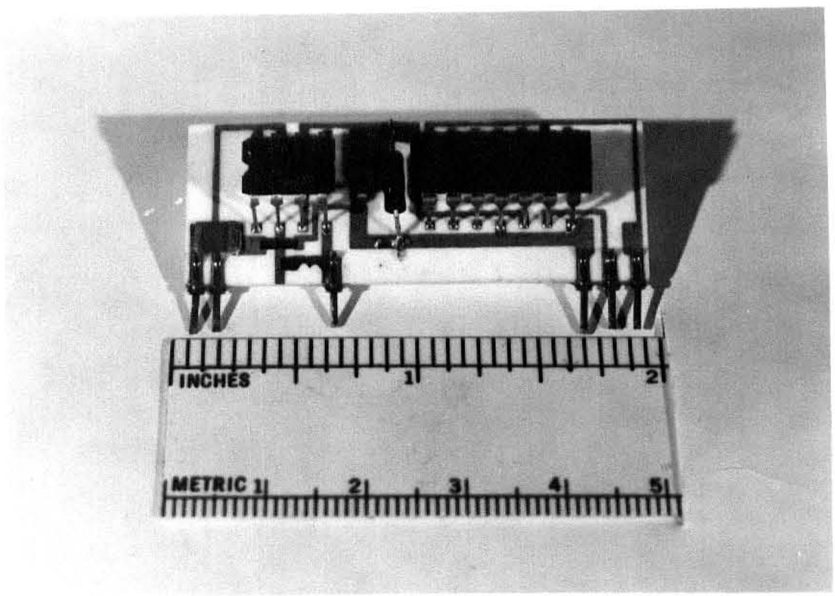

Figure 34. Thick film signal processing circuit before encapsulation.

struction. It can be encapsulated, making it impervious to dust and moisture.

In general, the thick film process involves printing conductors and resistors in paste form on a ceramic substrate using photographically reduced silk screen masks. The substrate is dried and then fired at eight hundred to one thousand degrees Centigrade, depending on the paste used. The values of the resistors can be adjusted by various trimming methods, and discrete components are then attached by reflow soldering. Due to the rigidity of the substrate and the small conductor size--twenty mil wide lines are easy to achieve--miniature components can often be employed. Finally, the substrate is encapsulated in epoxy for protection.

The circuit pictured in Figure 34 (before encapsulation) was produced in the facilities of the Department of Electrical Engineering at Kansas State University, and performed perfectly. It was assembled and R_2 and R_4 were functionally trimmed, that is, trimmed while the circuit was operating, to adjust the trigger level and the pulse length of the first monostable multivibrator. The circuits can be produced all alike and later adjusted by trimming for various applications. The trimming process is no more difficult than adjusting a potentiometer, but it requires some equipment and is not reversible.

CONCLUSION

On the basis of the calculations done for this study, it is not practical to monitor cylinder performance at the cylinder with cantilever beam devices. Beams of suitable size are subject to excitation by machine vibrations and plugging with straw, chaff, and dirt.

An impact type transducer has been developed which meets the design requirements. It is not susceptible to vibration, noise, dirt or moisture. It is small enough not to obstruct the operation of the combine. It can count approximately five times as fast as necessary if its output is modified by equations that were fitted, and its response can be considered linear to one-and-one-half to two times the design count rate.

The transducer is cheap enough to be practical as a commercial attachment, if further tests show it gives the desired information. Its output could be adapted to give an indication of bushels per hour on a dial or digital readout, or it could become part of a control system for the whole combine. For research, its output could be counted and stored for further study.

SUMMARY

The purpose of this research was to design a monitor which could detect cylinder loss in a combine. The design was based on Zaidi's finding that cylinder loss is related to the distribution of threshed grain under the concave. Monitoring cylinder loss by measuring the ratio of the amount of grain threshed at the front of the concave to the amount of grain threshed at the rear of the concave solved the problem of sampling the threshed straw for unthreshed heads and gave earlier warning of loss.

It was determined that measuring the mass flow of grain was impractical, so an impact counter was designed that counted individual kernels. Various materials and methods of attachment were studied to determine the best diaphragm, which was polyethylene mounted with silicone sealer. The counter was capable of counting about five times as fast as necessary, and was resistant to the noise, vibration, moisture and dirt found under the combine concave. It was also small enough not to obstruct the operation of the combine and fairly inexpensive.

The complete the counter, a circuit was designed to process its signals and make them compatible with electronic counters.

SUGGESTIONS FOR FURTHER RESEARCH

1. For this research to have any meaning, it is necessary for a combine to be equipped with these counters and tested in the field to determine if they work properly and give the information that they are designed to give.

2. If the preceeding is successful, the counters should be developed into practical attachments to improve the efficiency of grain combines.

3. If the transducers prove successful, but are too costly to develop for universal application, they could still be used to give insight into the operation of the combine cylinder on a research basis.

REFERENCES

American Society of Agricultural Engineers. 1973. Agricultural Engineer's Yearbook. St. Joseph, Michigan. American Society of Agricultural Engineers.

Arnold, R. E. 1964. Experiments with Rasp Bar Threshing Drums. Journal of Agricultural Engineering Research 9(2): 99-131.

Bolz, R. E. and Tuve, G. L. 1970. Handbook of Tables for Applied Engineering Science. Cleaveland, Ohio. Chemical Rubber Company.

Bredfeldt, R. T. 1968. Automatic Header Height Control for Self-Propelled Combines. Agricultural Engineering 49(11): 666-667.

Brumfield, K. 1970. Wheat Farming. New York, New York. Bonanza Books.

Byars, E. F. and Snyder, R. D. 1969. Engineering Mechanics of Deformable Bodies. Scranton, Pennsylvania. International Textbook Co.

Cooper, G. F. 1972. Concave Separation from Laboratory Tests. Transactions of the ASAE 15(5): 865-870.

Floyd, C. S. 1973. Scanning the 1973 North American Combine Market. Implement and Tractor 88(14): 7-8,31.

Friesen, O. H.; Zoerb, G. C.; and Bigsby, F. W. 1966. For Combines: Controlling Feed Rates Automatically. Agricultural Engineering 47(8) : 434-435.

Gayford, M. L. 1967. Electroacoustics. London, England. Newnes-Butterworths.

Grovum, M. A.; Krause, A. E.; and Reed, W. B. 1969. Combine Harvester Grain Loss Monitor. Agricultural Engineering 50(9): 525-525, 528.

Huntington, H. B. 1958. The Elastic Constants of Crystals. New York, New York. Academic Press.

Implement and Tractor. 1974. Combines--Self Propelled. Implement and Tractor 58th Annual Redbook 89(3): B_1, B_2, B_4, B_6.

Kaminski, T. L. and Zoerb, G. C. 1963. An Automatic Header Height Control for Grain Crops. Paper presented at the Winter Meeting of the ASAE. Paper No. 63-648.

Kepner, R. A.; Bainer, R.; and Barger, E. L. 1972. Principles of Farm Machinery. Westport, Connecticutt. A V I Publishing Co., Inc.

MacAulay, J. T. and Lee, J. H. A. 1969. Grain Separation on Oscillating Combine Sieves as Affected by Material Entrance Conditions. Transactions of the ASAE 12(5) : 648-651, 654.

Melen, R. and Garland, H. 1971. I C Operational Amplifiers. Indianapolis, Indiana. Howard W. Sams and Company.

Nyborg, E. O.; McColly, R. T.; and Hinkle, R. T. 1968. Grain Combine Loss Characteristics. Paper presented at the Winter Meeting of the ASAE.

Ogata, K. 1970. Modern Control Engineering. Englewood Cliffs, New Jersey. Prentice Hall, Inc.

Perry, C. C. and Lissner, H. R. 1955. The Strain Gage Primer. New York, New York. McGraw-Hill Book Company, Inc.

Rumble, D. W. and Lee, J. H. A. 1970. Aerodynamic Separation in a Combine Shoe. Transactions of the ASAE 13(1): 6-8.

Snedecor, G. W. and Cochran, W. G. 1967. Statistical Methods. Ames, Iowa. Iowa State University Press.

Story, A. G.; Johnson, W. H.; and Stewart, R. E. 1968. Remote Measurement of Concentration and Height of Heads of Standing Grain with Microwave Energy. Paper presented at the Annual Meeting of the ASAE. Logan, Utah. Paper No. 68-113.

Thompson, W. T. 1972. Theory of Vibrations. Englewood Cliffs, New Jersey. Prentice-Hall Inc.

Zaidi, S. H. 1974. A Comparison of Five Wheat Threshability Parameters Using an Instrumented Laboratory Cylinder. Unpublished M. S. Thesis. Kansas State University Library. Manhattan, Kansas.

Appendix A

The design of the size of the cantelever beam proceeds in reverse order. A final maximum output voltage of six volts is desired. With a gain of one thousand, .006 volts is required from the strain gage bridge.

$$\Delta e = \frac{E \, \Delta R}{R} \qquad (1) \text{ Perry and Lissner (1955)}$$

Δe, volts, output of the strain gage bridge; E, volts, bridge excitation voltage; ΔR, ohms, change in gage resistance due to strain; R, ohms, nominal gage resistance.

$$.006 = \frac{6 \, \Delta R}{120}$$

$$.12 = \Delta R$$

$$\frac{\Delta R}{R} = F \frac{\Delta L}{L} \qquad (2) \text{ Perry and Lissner (1955)}$$

F, dimensionless, gage factor; $\frac{\Delta L}{L}$, inches per inch, strain.

$$\frac{.12}{120} = 2.00 \frac{\Delta L}{L}$$

$$.0005 = \frac{\Delta L}{L}$$

Appendix A (continued)

$$\frac{\Delta L}{L} = \frac{M\ u}{E\ I}$$ (3) Byars and Snyder (1969)

M, inch-pounds, distance from point of application of load to point of measurement of stress times load; u, inches, distance from neutral axis of beam to point of measurement, in this case the beam thickness divided by two; E, pounds per square inch, the modulus of elasticity for steel, 29×10^6 psi; I, inches^4, moment of inertia, $\frac{1}{12} b\ t^3$, where b is the width of the beam in inches and t is the thickness of the beam in inches.

For this example use a load of .0142 pounds, from Figure 1; distance from point of application of load to point of measurement of stress, 4.5 inches, assuming a maximum beam length of five inches due to restrictions on the size of the device; and the minimum beam width that will still permit mounting gages, .25 inches.

$$.0005 = \frac{.0142 \times 4.5 \times \frac{t}{2}}{29 \times 10^6 \times \frac{1}{12} \times t^3}$$

$$t = .00514$$

$$K = \frac{E \times b \times t^3}{4\ l^3}$$ (4) Thompson (1972)

K, pounds per inch, spring constant; l, inches, length of beam.

$$K = \frac{29 \times 10^6 \times .25 \times .00514^3}{4 \times 5^3}$$

$$K = .00197$$

Appendix A (continued)

The mass of the pan, 2 inches by 2 inches by .025 inches, aluminum, is .1 $inch^3$ times 2.73, the specific gravity of aluminum, times .036 pounds per $inch^3$, density of water, which is .009858 pounds.

$$\omega_n = \sqrt{\frac{K}{M}} \qquad \text{(5) Thompson (1972)}$$

M, slugs, mass of the pan plus the mass of the wheat on the pan, .0142 pounds plus .009858 pounds divided by 32.2 pounds per slug, .000747 slugs. ω_n, radians per second, natural frequency.

$$\omega_n = \sqrt{\frac{.00197}{.000747}}$$

ω_n = 1.624 rad/sec or 15.5 rev/min.

Appendix B

The determination of the maximum permissible pulse length on the basis of the probability of overlapping counts depends on the assumption that the incidence of the kernels on the counter is a Poisson distribution. This assumption accepted, the determination proceeds as follows.

There is at least one error if two or more kernels strike the transducer in one pulse width. The probability of two or more strikes in a period of time is one minus the probability of one or zero strikes in a period of time.

$$P\ [2 \text{ or more in T sec.}] = 1 - P\ [1 \text{ or } 0 \text{ in T sec.}]$$

$$P\ [2 \text{ or more in T sec.}] = 1 - P\ [1] - P\ [0]$$

The probability of exactly k strikes in T seconds;

$$P\ [\text{exactly k in T sec.}] = \frac{(\lambda T)^k}{k!} e^{-\lambda T} \qquad (6)$$ Snedecor and Cochran (1967)

λ, the average number of kernels in T seconds; T, the pulse length; and k, the number of strikes.

$$P\ [2 \text{ or more in T sec.}] = 1 - \frac{(\lambda T)^1}{1!} e^{-\lambda T} - \frac{(\lambda T)^0}{0!} e^{-\lambda T}$$

$$\text{"} \qquad = 1 - \lambda T\, e^{-\lambda T} - e^{-\lambda T}$$

$$\text{"} \qquad = 1 - e^{-\lambda T} (\lambda T + 1)$$

This relationship was used to calculate the probabilities of error for different flow rates and pluse lengths shown in Figure 5.

The predicted performance in Figures 24, 25, and 26 was developed from the same theory in the following manner.

Appendix B (continued)

$$P\,[1 \text{ or more in } T \text{ sec.}] = 1 - P\,[0 \text{ in } T \text{ sec.}]$$

$$\text{"} \quad = 1 - \frac{(\lambda T)^0}{0!}\, e^{-\lambda T}$$

$$\text{"} \quad = 1 - e^{-\lambda T}$$

This probability, times the number of T second periods in a minute, gave the predicted performance.

Appendix C

Polyethylene Diaphragm, Elastically Mounted, Center Impacts.

Impact No.	Diaphragm Number 1		2		3		4		5	
	H	L	H	L	H	L	H	L	H	L
1	10	2.0	11	1.6	9	1.8	12	1.8	10	1.6
2	9	2.0	10	1.6	12	1.8	11	1.8	12	1.6
3	10	2.0	10	1.6	12	1.8	11	1.8	12	1.6
4	8	2.0	10	1.6	12	1.8	12	1.8	10	1.6
5	9	2.0	11	1.6	12	1.8	13	1.8	11	1.6
6	10	2.0	13	1.6	12	1.8	13	1.8	12	1.6
7	9	2.0	11	1.6	12	1.8	12	1.8	11	1.6
8	9	2.0	12	1.6	12	1.8	12	1.8	10	1.6
9	10	2.0	12	1.6	11	1.8	11	1.8	10	1.6
10	9	2.0	10	1.6	12	1.8	13	1.8	10	1.6
$\bar{x}$	9.3		11.0		11.6		12.2		10.5	
s	.67		1.05		.97		.79		.71	

Mean of $\bar{x}$'s = 10.92, Standard Deviation os $\bar{x}$'s = 1.11.

Polyethylene Diaphragm, Inelastically Mounted, Center Impacts.

Impact No.	Diaphragm Number 1		2		3		4		5	
	H	L	H	L	H	L	H	L	H	L
1	5.5	1.0	6.0	1.0	7.5	1.2	7.0	1.2	3.0	.8
2	6.0	1.0	6.0	1.0	7.0	1.2	6.5	1.2	3.0	.8
3	5.5	1.0	5.5	1.0	8.0	1.2	7.0	1.2	4.0	.8
4	6.0	1.0	5.5	1.0	8.0	1.2	6.5	1.2	4.0	.8
5	6.0	1.0	6.0	1.0	8.0	1.2	6.5	1.2	4.5	.8
6	5.5	1.0	6.0	1.0	7.0	1.2	6.5	1.2	4.0	.8
7	6.0	1.0	5.5	1.0	7.0	1.2	7.0	1.2	4.0	.8
8	6.0	1.0	6.0	1.0	7.0	1.2	6.5	1.2	4.0	.8
9	6.0	1.0	6.0	1.0	8.0	1.2	7.0	1.2	4.0	.8
10	6.0	1.0	6.0	1.0	7.0	1.2	7.0	1.2	4.0	.8
$\bar{x}$	5.85		5.85		7.45		6.75		3.85	
s	.24		.24		.50		.26		.47	

Mean of $\bar{x}$'s = 5.95, Standard Deviation of $\bar{x}$'s = 1.35.

H indicates maximum pulse height in volts, L indicates pulse length in msec.

Appendix C (continued)

Aluminum Diaphragm, Elastically Mounted, Center Impacts.

Impact No.	1 H	1 L	2 H	2 L	3 H	3 L	4 H	4 L	5 H	5 L
1	3.6	1.0	2.9	1.0	3.8	1.2	2.9	1.0	2.0	.75
2	3.5	1.0	2.5	1.0	3.7	1.2	3.0	1.0	2.0	.75
3	3.4	1.0	2.5	1.0	3.5	1.2	3.2	1.0	2.0	.75
4	3.1	1.0	2.9	1.0	3.8	1.2	3.0	1.0	2.2	.75
5	3.5	1.0	2.8	1.0	3.7	1.2	3.0	1.0	2.2	.75
6	3.3	1.0	2.8	1.0	4.0	1.2	3.0	1.0	2.2	.75
7	3.6	1.0	2.7	1.0	3.9	1.2	3.1	1.0	2.0	.75
8	3.4	1.0	2.8	1.0	3.8	1.2	3.2	1.0	2.1	.75
9	3.2	1.0	2.7	1.0	3.6	1.2	3.0	1.0	2.0	.75
10	3.5	1.0	2.4	1.0	3.3	1.2	2.8	1.0	2.0	.75
$\bar{x}$	3.41		2.70		3.71		3.02		2.07	
s	..17		..18		.20		.12		.09	

Mean of $\bar{x}$'s = 2.98, Standard Deviation of $\bar{x}$'s = .64.

Aluminum Diaphragm, Inelastically Mounted, Center Impacts.

Impact No.	1 H	1 L	2 H	2 L	3 H	3 L	4 H	4 L	5 H	5 L
1	.8	.7	1.6	.4	.6	.7	1.6	1.0	.4	.1
2	1.0	.7	1.8	.4	.5	.7	1.5	1.0	.5	.1
3	.9	.7	2.0	.4	.7	.7	1.5	1.0	.4	.1
4	.9	.7	1.9	.4	.6	.7	1.5	1.0	.3	.1
5	.8	.7	2.0	.4	.7	.7	1.6	1.0	.5	.1
6	.9	.7	2.0	.4	.7	.7	1.6	1.0	.4	.1
7	.9	.7	2.0	.4	.7	.7	1.5	1.0	.4	.1
8	.9	.7	2.0	.4	.7	.7	1.7	1.0	.3	.1
9	1.0	.7	2.1	.4	.6	.7	1.6	1.0	.4	.1
10	.9	.7	2.0	.4	.7	.7	1.6	1.0	.3	.1
$\bar{x}$	.89		1.94		.65		1.57		.39	
s	.07		.14		.07		.07		.07	

Mean of $\bar{x}$'s = 1.09, Standard Deviation of $\bar{x}$'s = .59.

H indicates maximum pulse height in volts, L indicates pulse length in msec.

Appendix C (continued)

Steel Diaphragm, Elastically Mounted, Center Impacts.

Impact No.	Diaphragm Number 1 H	1 L	2 H	2 L	3 H	3 L	4 H	4 L	5 H	5 L
1	.9	1.5	.9	.4	.9	.9	1.0	.5	1.0	.6
2	.8	1.5	.9	.4	.8	.9	.9	.5	.9	.6
3	.8	1.5	.7	.4	.7	.9	.9	.5	1.0	.6
4	.8	1.5	.9	.4	.8	.9	.7	.5	.9	.6
5	.8	1.5	.8	.4	.8	.9	.9	.5	1.0	.6
6	.8	1.5	.9	.4	.8	.9	.9	.5	1.0	.6
7	.9	1.5	.9	.4	.9	.9	1.0	.5	.8	.6
8	.8	1.5	.8	.4	.9	.9	.9	.5	.9	.6
9	.8	1.5	.9	.4	.8	.9	.9	.5	.9	.6
10	.8	1.5	.9	.4	.8	.9	.9	.5	.9	.6
$\bar{x}$	.82		.86		.82		.90		.93	
s	.04		.07		.06		.08		.07	

Mean of $\bar{x}$'s = .87, Standard Deviation of $\bar{x}$'s = .05.

Steel Diaphragm, Inelastically Mounted, Center Imapcts.

Impacts No.	Diaphragm Number 1 H	1 L	2 H	2 L	3 H	3 L	4 H	4 L	5 H	5 L
1	.6	1.0	.8	1.5	1.0	1.0	.8	.5	.8	1.0
2	.6	1.0	.9	1.5	1.0	1.0	.9	.5	.7	1.0
3	.6	1.0	.9	1.5	1.0	1.0	.7	.5	.7	1.0
4	.6	1.0	.8	1.5	.8	1.0	.8	.5	.6	1.0
5	.6	1.0	.7	1.5	1.0	1.0	.9	.5	.7	1.0
6	.6	1.0	.8	1.5	.7	1.0	.9	.5	.7	1.0
7	.6	1.0	.7	1.5	.9	1.0	.9	.5	.6	1.0
8	.6	1.0	.8	1.5	.8	1.0	.9	.5	.8	1.0
9	.6	1.0	.7	1.5	.9	1.0	.9	.5	.8	1.0
10	.7	1.0	.8	1.5	1.0	1.0	.8	.5	.7	1.0
$\bar{x}$	.61		.79		.91		.85		.71	
s	.03		.07		.11		.07		.07	

Mean of $\bar{x}$'s = .77, Standard Deviation of $\bar{x}$'s = .12.

H indicates maximum pulse height in volts, L indicates pulse length in msec.

Appendix C (continued)

Copper Diaphragm, Elastically Mounted, Center Impacts.

Impact No.	1 H	1 L	2 H	2 L	3 H	3 L	4 H	4 L	5 H	5 L
	Diaphragm Number									
1	1.2	2.0	1.5	1.8	1.0	2.0	1.2	1.0	1.4	1.0
2	1.5	2.0	1.7	1.8	1.4	2.0	1.3	1.0	1.3	1.0
3	1.1	2.0	1.6	1.8	1.3	2.0	1.0	1.0	1.2	1.0
4	1.3	2.0	1.7	1.8	1.3	2.0	1.1	1.0	1.4	1.0
5	1.4	2.0	1.8	1.8	1.4	2.0	1.3	1.0	1.4	1.0
6	1.3	2.0	1.7	1.8	1.2	2.0	1.1	1.0	1.4	1.0
7	1.3	2.0	1.7	1.8	1.3	2.0	1.3	1.0	1.3	1.0
8	1.4	2.0	1.7	1.8	1.1	2.0	1.2	1.0	1.0	1.0
9	1.5	2.0	1.7	1.8	1.4	2.0	1.1	1.0	1.4	1.0
10	1.3	2.0	1.6	1.8	1.3	2.0	1.2	1.0	1.4	1.0
$\bar{x}$	1.33		1.67		1.27		1.18		1.32	
s	.13		.08		.13		.10		.13	

Mean of $\bar{x}$'s = 1.35, Standard Deviation of $\bar{x}$'s = .19.

Copper Diaphragm, Inelastically Mounted, Center Impacts.

Impact No.	1 H	1 L	2 H	2 L	3 H	3 L	4 H	4 L	5 H	5 L
	Diaphragm Number									
1	.5	3.0	.7	4.0	.4	4.0	.6	4.0	.7	4.0
2	.4	3.0	.7	4.0	.6	4.0	.6	4.0	.7	4.0
3	.5	3.0	.6	4.0	.7	4.0	.6	4.0	.7	4.0
4	.5	3.0	.6	4.0	.7	4.0	.6	4.0	.7	4.0
5	.6	3.0	.6	4.0	.6	4.0	.6	4.0	.7	4.0
6	.5	3.0	.6	4.0	.7	4.0	.6	4.0	.7	4.0
7	.5	3.0	.7	4.0	.7	4.0	.6	4.0	.7	4.0
8	.5	3.0	.6	4.0	.6	4.0	.5	4.0	.7	4.0
9	.5	3.0	.6	4.0	.7	4.0	.6	4.0	.8	4.0
10	.5	3.0	.6	4.0	.6	4.0	.5	4.0	.7	4.0
$\bar{x}$	.50		.63		.63		.57		.71	
s	.05		.05		.09		.05		.03	

Mean of $\bar{x}$'s = .61, Standard Deviation of $\bar{x}$'s = .06.

H indicates maximum pulse height in volts, L indicates pulse length in msec.

Appendix C (continued)

Polyethylene Diaphragm, Elastically Mounted, Impacts .16 Inch from Center.

Impact No.	Diaphragm Number 1		2		3		4		5	
	H	L	H	L	H	L	H	L	H	L
1	5.0	.7	5.5	.2	3.5	1.2	5.0	.3	6.0	.3
2	5.0	.7	5.0	.2	4.0	1.2	5.5	.3	6.0	.3
3	5.0	.7	6.0	.2	4.0	1.2	5.0	.3	5.0	.3
4	5.0	.7	6.0	.2	4.0	1.2	5.5	.3	5.8	.3
5	4.9	.7	6.2	.2	4.0	1.2	5.0	.3	6.0	.3
6	5.0	.7	6.0	.2	4.0	1.2	5.0	.3	5.0	.3
7	5.0	.7	6.0	.2	4.0	1.2	5.0	.3	6.0	.3
8	5.0	.7	6.0	.2	3.0	1.2	5.0	.3	5.8	.3
9	5.0	.7	5.8	.2	4.4	1.2	5.0	.3	6.0	.3
10	5.0	.7	5.8	.2	4.2	1.2	5.2	.3	5.5	.3
$\bar{x}$	4.99		5.83		3.91		5.12		5.71	
s	.03		.35		.39		.21		.41	

Mean of $\bar{x}$'s = 5.11, Standard Deviation of $\bar{x}$'s = .76.

Polyethylene Diaphragm, Inelastically Mounted, Impacts .16 Inch from Center.

Impact No.	Diaphragm Number 1		2		3		4		5	
	H	L	H	L	H	L	H	L	H	L
1	3.5	2.0	4.0	1.5	4.0	1.5	5.0	1.5	2.2	1.0
2	3.5	2.0	3.8	1.5	3.5	1.5	5.0	1.5	2.8	1.0
3	3.0	2.0	4.0	1.5	3.5	1.5	5.0	1.5	1.3	1.0
4	3.5	2.0	3.8	1.5	4.2	1.5	5.0	1.5	2.2	1.0
5	3.8	2.0	3.5	1.5	3.8	1.5	5.0	1.5	2.4	1.0
6	3.2	2.0	4.1	1.5	4.2	1.5	5.0	1.5	2.3	1.0
7	3.5	2.0	4.2	1.5	2.8	1.5	5.5	1.5	2.5	1.0
8	3.5	2.0	4.0	1.5	4.0	1.5	5.0	1.5	2.1	1.0
9	3.5	2.0	4.0	1.5	3.8	1.5	5.0	1.5	2.0	1.0
10	3.5	2.0	4.0	1.5	3.8	1.5	5.0	1.5	2.6	1.0
$\bar{x}$	3.45		3.94		3.86		5.05		2.34	
s	.21		.20		.25		.16		.24	

Mean of $\bar{x}$'s = 3.73, Standard Deviation of $\bar{x}$'s = .98.

H indicates maximum pulse height in volts, L indicates pulse length in msec.

Appendix C (continued)

Aluminum Diaphragm, Elastically Mounted, Impacts .16 Inch from Center.

Impact No.	Diaphragm Number 1		2		3		4		5	
	H	L	H	L	H	L	H	L	H	L
1	1.8	2.0	2.2	1.3	3.0	2.0	3.0	2.0	2.8	1.5
2	3.2	2.0	2.5	1.3	3.4	2.0	3.0	2.0	2.2	1.5
3	2.6	2.0	2.2	1.3	3.2	2.0	3.0	2.0	2.8	1.5
4	3.2	2.0	2.4	1.3	3.0	2.0	3.0	2.0	2.5	1.5
5	3.2	2.0	2.0	1.3	3.4	2.0	3.0	2.0	2.5	1.5
6	3.2	2.0	2.0	1.3	3.5	2.0	3.2	2.0	2.4	1.5
7	3.2	2.0	2.6	1.3	3.2	2.0	3.2	2.0	2.5	1.5
8	3.2	2.0	2.4	1.3	3.4	2.0	3.0	2.0	3.0	1.5
9	3.2	2.0	2.5	1.3	3.4	2.0	3.2	2.0	2.6	1.5
10	3.3	2.0	2.5	1.3	3.4	2.0	3.0	2.0	2.2	1.5
$\bar{x}$	3.01		2.33		3.29		3.06		2.55	
s	.47		.22		.18		.10		.26	

Mean of $\bar{x}$'s = 2.65, Standard Deviation of $\bar{x}$'s = .99.

Aluminum Diaphragm, Inelastically Mounted, Impacts .16 Inch from Center.

Impact No.	Diaphragm Number 1		2		3		4		5	
	H	L	H	L	H	L	H	L	H	L
1	.4	1.5	.7	.5	.4	1.5	1.2	1.5	.30	.5
2	.5	1.5	.7	.5	.4	1.5	1.0	1.5	.30	.5
3	.5	1.5	.7	.5	.4	1.5	.9	1.5	.30	.5
4	.5	1.5	.7	.5	.4	1.5	1.0	1.5	.25	.5
5	.5	1.5	.7	.5	.4	1.5	.9	1.5	.30	.5
6	.4	1.5	.6	.5	.4	1.5	.9	1.5	.25	.5
7	.5	1.5	.6	.5	.4	1.5	1.0	1.5	.20	.5
8	.4	1.5	.7	.5	.4	1.5	.8	1.5	.30	.5
9	.4	1.5	.7	.5	.4	1.5	.7	1.5	.30	.5
10	.5	1.5	.8	.5	.4	1.5	1.0	1.5	.30	.5
$\bar{x}$	.46		.69		.40		.94		.28	
s	.05		.06		.00		.13		.03	

Mean of $\bar{x}$'s = .55, Standard Deviation of $\bar{x}$'s = .26.

H indicates maximum pulse height in volts, L indicates pulse length in msec.

Appendix C (continued)

Steel Diaphragm, Elastically Mounted, Impacts .16 Inch from Center.

Impact No.	Diaphragm Number 1		2		3		4		5	
	H	L	H	L	H	L	H	L	H	L
1	1.2	1.5	.5	.5	1.0	3.0	1.0	2.0	.9	.5
2	1.2	1.5	.6	.5	1.2	3.0	.9	2.0	.7	.5
3	1.0	1.5	.6	.5	1.0	3.0	1.0	2.0	.8	.5
4	1.0	1.5	.6	.5	1.1	3.0	1.0	2.0	.7	.5
5	1.2	1.5	.8	.5	1.1	3.0	1.1	2.0	.6	.5
6	1.0	1.5	.8	.5	1.1	3.0	1.0	2.0	.7	.5
7	1.0	1.5	.8	.5	1.1	3.0	1.0	2.0	.7	.5
8	1.0	1.5	.8	.5	1.0	3.0	.9	2.0	.8	.5
9	1.2	1.5	.8	.5	1.0	3.0	1.0	2.0	.6	.5
10	1.2	1.5	.7	.5	1.0	3.0	1.1	2.0	.7	.5
$\bar{x}$	1.10		.70		1.04		1.00		.72	
s	.11		.11		.08		.07		.09	

Mean of $\bar{x}$'s = .91, Standard Deviation of $\bar{x}$'s = .19.

Steel Diaphragm, Inelastically Mounted, Impacts .16 Inch from Center.

Impact No.	Diaphragm Number 1		2		3		4		5	
	H	L	H	L	H	L	H	L	H	L
1	.7	.5	1.3	2.0	1.0	1.0	1.1	.5	.6	.5
2	.7	.5	1.5	2.0	.8	1.0	1.1	.5	.7	.5
3	.7	.5	1.5	2.0	.9	1.0	1.2	.5	.7	.5
4	.6	.5	1.4	2.0	.8	1.0	1.3	.5	.7	.5
5	.7	.5	1.3	2.0	1.0	1.0	1.1	.5	.8	.5
6	.8	.5	1.4	2.0	1.0	1.0	1.1	.5	.8	.5
7	.7	.5	1.3	2.0	1.0	1.0	1.2	.5	.7	.5
8	.8	.5	1.5	2.0	1.1	1.0	1.1	.5	.7	.5
9	.7	.5	1.4	2.0	1.0	1.0	1.0	.5	.8	.5
10	.8	.5	1.3	2.0	1.1	1.0	1.0	.5	.7	.5
$\bar{x}$	.72		1.39		.97		1.12		.72	
s	.06		.09		.11		.09		.06	

Mean of $\bar{x}$'s = .98, Standard Deviation of $\bar{x}$'s = .28.

H indicates maximum pulse height in volts, L indicates pulse length in msec.

Appendix C (continued)

Copper Diaphragm, Elastically Mounted, Impacts .16 Inch from Center.

Impact No.	Diaphragm Number 1		2		3		4		5	
	H	L	H	L	H	L	H	L	H	L
1	.8	1.5	.8	3.0	.6	3.0	.7	2.0	.8	2.0
2	.8	1.5	.8	3.0	.6	3.0	.7	2.0	.8	2.0
3	.8	1.5	.7	3.0	.6	3.0	.5	2.0	.7	2.0
4	.8	1.5	.7	3.0	.6	3.0	.6	1.5	.7	2.0
5	.8	1.5	.8	3.0	.6	3.0	.5	1.5	.8	2.0
6	.8	1.5	.8	3.0	.6	3.0	.5	1.5	.8	2.0
7	.8	1.5	.7	3.0	.6	3.0	.6	1.5	.7	2.0
8	.8	1.5	.7	3.0	.6	3.0	.6	1.5	.7	2.0
9	.8	1.5	.8	3.0	.6	3.0	.6	1.5	.6	2.0
10	.8	1.5	.7	3.0	.6	3.0	.5	1.5	.7	2.0
$\bar{x}$	.8		.75		.6		.57		.71	
s	0		.05		0		.07		.07	

Mean of $\bar{x}$'s = .69, Standard Deviation of $\bar{x}$'s = .10.

Copper Diaphragm, Inelastically Mounted, Impacts .16 Inch from Center.

Impact No.	Diaphragm Number 1		2		3		4		5	
	H	L	H	L	H	L	H	L	H	L
1	.35	2.0	.35	2.0	.40	3.0	.35	3.0	.40	2.0
2	.35	2.0	.35	2.0	.30	3.0	.35	3.0	.40	2.0
3	.35	2.0	.30	2.0	.40	3.0	.32	3.0	.35	2.0
4	.30	2.0	.30	2.0	.40	3.0	.35	3.0	.30	2.0
5	.30	2.0	.38	2.0	.35	3.0	.30	3.0	.32	2.0
6	.35	2.0	.30	2.0	.40	3.0	.35	3.0	.35	2.0
7	.32	2.0	.30	2.0	.35	3.0	.30	3.0	.35	2.0
8	.35	2.0	.32	2.0	.30	3.0	.35	3.0	.32	2.0
9	.30	2.0	.35	2.0	.30	3.0	.37	3.0	.35	2.0
10	.35	2.0	.30	2.0	.35	3.0	.32	3.0	.35	2.0
$\bar{x}$	.33		.33		.36		.34		.35	
s	.02		.03		.04		.02		.03	

Mean of $\bar{x}$'s = .34, Standard Deviation of $\bar{x}$'s = .01.

H indicates maximum pulse height in volts, L indicates pulse length in msec.

Appendix C (continued)

Polyethylene Diaphragm, Elastically Mounted, Impacts .32 Inch from Center.

Impact No.	Diaphragm Number 1		2		3		4		5	
	H	L	H	L	H	L	H	L	H	L
1	1.7	3.0	1.5	2.0	1.8	2.0	2.0	3.0	1.7	2.5
2	1.9	3.0	1.5	2.0	1.6	2.0	2.0	3.0	2.0	2.5
3	2.0	3.0	1.6	2.0	2.0	2.0	2.0	3.0	1.5	2.5
4	2.0	3.0	1.7	2.0	2.0	2.0	2.0	3.0	1.6	2.5
5	1.8	3.0	1.6	2.0	1.5	2.0	2.0	3.0	1.5	2.5
6	2.1	3.0	1.6	2.0	2.0	2.0	2.2	3.0	1.5	2.5
7	2.0	3.0	1.7	2.0	2.0	2.0	2.0	3.0	1.5	2.5
8	2.2	3.0	1.6	2.0	2.0	2.0	2.0	3.0	1.6	2.5
9	2.2	3.0	1.5	2.0	2.0	2.0	2.0	3.0	1.6	2.5
10	2.2	3.0	1.8	2.0	2.0	2.0	2.0	3.0	1.5	2.5
$\bar{x}$	2.01		1.61		1.89		2.02		1.60	
s	.17		.19		.06		.06		.16	

Mean of $\bar{x}$'s = 1.83, Standard Deviation of $\bar{x}$'s = .21.

Polyethylene Diaphragm, Inelastically Mounted, Impacts .32 Inch from Center.

Impact No.	Diaphragm Number 1		2		3		4		5	
	H	L	H	L	H	L	H	L	H	L
1	1.0	1.0	.7	1.0	.9	1.0	.8	1.0	.7	1.0
2	.7	1.0	.8	1.0	.8	1.0	1.0	1.0	.8	1.0
3	.9	1.0	.8	1.0	.6	1.0	.9	1.0	.7	1.0
4	1.1	1.0	.8	1.0	.6	1.0	.7	1.0	.7	1.0
5	1.0	1.0	.6	1.0	.9	1.0	.7	1.0	.6	1.0
6	.8	1.0	.7	1.0	.8	1.0	.9	1.0	.5	1.0
7	.9	1.0	.8	1.0	1.0	1.0	.8	1.0	.6	1.0
8	.7	1.0	1.0	1.0	1.0	1.0	.6	1.0	.7	1.0
9	.9	1.0	.8	1.0	1.0	1.0	.8	1.0	.7	1.0
10	1.0	1.0	.9	1.0	1.0	1.0	.8	1.0	.7	1.0
$\bar{x}$	.90		.79		.86		.80		.64	
s	.13		.11		.16		.12		.16	

Mean of $\bar{x}$'s = .80, Standard Deviation of $\bar{x}$'s = .10.

H indicates maximum pulse height in volts, L indicates pulse length in msec.

Appendix C (continued)

Aluminum Diaphragm, Elastically Mounted, Impacts .32 Inch from Center.

Impact No.	1 H	1 L	2 H	2 L	3 H	3 L	4 H	4 L	5 H	5 L
1	.8	2.0	.7	1.0	.8	1.0	.8	2.5	.7	1.0
2	.9	2.0	.8	1.0	.7	1.0	1.0	2.5	.6	1.0
3	.7	2.0	.8	1.0	.8	1.0	1.1	2.5	.6	1.0
4	.9	2.0	.6	1.0	.8	1.0	1.4	2.5	.6	1.0
5	.9	2.0	.6	1.0	.8	1.0	1.4	2.5	.6	1.0
6	.6	2.0	.9	1.0	.7	1.0	1.1	2.5	.7	1.0
7	.7	2.0	.7	1.0	.9	1.0	.9	2.5	.7	1.0
8	.8	2.0	.6	1.0	.8	1.0	1.0	2.5	.6	1.0
9	.7	2.0	.7	1.0	1.1	1.0	1.2	2.5	.6	1.0
10	.7	2.0	.7	1.0	1.0	1.0	1.3	2.5	.6	1.0
$\bar{x}$	.77		.71		.78		1.08		.63	
s	.11		.09		.19		.18		.05	

Mean of $\bar{x}$'s = .79, Standard Deviation of $\bar{x}$'s = .17.

Aluminum Diaphragm, Inelastically Mounted, Impacts .32 Inch from Center.

Impact No.	1 H	1 L	2 H	2 L	3 H	3 L	4 H	4 L	5 H	5 L
1	.10	2.5	.17	3.0	.15	4.0	.16	2.0	.12	2.5
2	.12	2.5	.17	3.0	.12	4.0	.19	2.0	.08	2.5
3	.08	2.5	.16	3.0	.10	4.0	.20	2.0	.13	2.5
4	.12	2.5	.15	3.0	.15	4.0	.18	2.0	.08	2.5
5	.09	2.5	.18	3.0	.20	4.0	.15	2.0	.11	2.5
6	.17	2.5	.20	3.0	.16	4.0	.10	2.0	.08	2.5
7	.16	2.5	.17	3.0	.10	4.0	.20	2.0	.11	2.5
8	.15	2.5	.20	3.0	.07	4.0	.20	2.0	.07	2.5
9	.15	2.5	.15	3.0	.08	4.0	.10	2.0	.10	2.5
10	.18	2.5	.16	3.0	.15	4.0	.20	2.0	.10	2.5
$\bar{x}$	.13		.17		.13		.17		.10	
s	.03		.02		.04		.04		.02	

Mean of $\bar{x}$'s = .14, Standard Deviation of $\bar{x}$'s = .03

H indicates maximum pulse height in volts, L indicates pulse length in msec.

Appendix C (continued)

Steel Diaphragm, Elastically Mounted, Impacts .32 Inch from Center.

Impact No.	Diaphragm Number 1		2		3		4		5	
	H	L	H	L	H	L	H	L	H	L
1	.30	3.0	.20	1.0	.40	1.5	.30	1.0	.25	.5
2	.22	3.0	.15	1.0	.30	1.5	.30	1.0	.35	.5
3	.36	3.0	.25	1.0	.30	1.5	.32	1.0	.32	.5
4	.28	3.0	.20	1.0	.25	1.5	.30	1.0	.24	.5
5	.32	3.0	.15	1.0	.25	1.5	.30	1.0	.30	.5
6	.30	3.0	.15	1.0	.30	1.5	.36	1.0	.30	.5
7	.22	3.0	.13	1.0	.30	1.5	.30	1.0	.32	.5
8	.25	3.0	.20	1.0	.30	1.5	.30	1.0	.24	.5
9	.36	3.0	.16	1.0	.30	1.5	.26	1.0	.32	.5
10	.38	3.0	.18	1.0	.30	1.5	.30	1.0	.24	.5
$\bar{x}$	.30		.18		.30		.31		.29	
s	.06		.04		.04		.02		.04	

Mean of $\bar{x}$'s = .29, Standard Deviation of $\bar{x}$'s = .05.

Steel Diaphragm, Inelastically Mounted, Impacts .32 Inch from Center.

Impact No.	Diaphragm Number 1		2		3		4		5	
	H	L	H	L	H	L	H	L	H	L
1	.13	1.0	.14	1.0	.16	1.0	.25	1.0	2.0	1.0
2	.14	1.0	1.5	1.0	.10	1.0	.20	1.0	1.0	1.0
3	.11	1.0	.17	1.0	.17	1.0	.32	1.0	2.5	1.0
4	.13	1.0	.17	1.0	.17	1.0	.28	1.0	1.0	1.0
5	.07	1.0	.14	1.0	.16	1.0	.28	1.0	2.0	1.0
6	.15	1.0	.15	1.0	.16	1.0	.25	1.0	2.4	1.0
7	.11	1.0	.14	1.0	.19	1.0	.24	1.0	1.5	1.0
8	.11	1.0	.16	1.0	.18	1.0	.32	1.0	1.0	1.0
9	.13	1.0	.15	1.0	.16	1.0	.24	1.0	1.0	1.0
10	.10	1.0	.14	1.0	.13	1.0	.30	1.0	1.0	1.0
$\bar{x}$	.12		.15		.16		.27		1.54	
s	.02		.01		.03		.04		.63	

Mean of $\bar{x}$'s = .45, Standard Deviation of $\bar{x}$'s = .61.

H indicates maximum pulse height in volts, L indicates pulse length in msec.

Appendix C (continued)

Copper Diaphragm, Elastically Mounted, Impacts .32 Inch from Center.

Impact No.	Diaphragm Number 1		2		3		4		5	
	H	L	H	L	H	L	H	L	H	L
1	.15	5.0	.10	4.0	.10	2.5	.16	4.0	.15	3.0
2	.15	5.0	.18	4.0	.10	2.5	.16	4.0	.15	3.0
3	.12	5.0	.19	4.0	.09	2.5	.15	4.0	.17	3.0
4	.13	5.0	.20	4.0	.10	2.5	.14	4.0	.13	3.0
5	.13	5.0	.20	4.0	.09	2.5	.13	4.0	.16	3.0
6	.14	5.0	.20	4.0	.10	2.5	.15	4.0	.17	3.0
7	.13	5.0	.20	4.0	.10	2.5	.15	4.0	.18	3.0
8	.13	5.0	.19	4.0	.10	2.5	.15	4.0	.20	3.0
9	.13	5.0	.15	4.0	.10	2.5	.12	4.0	.15	3.0
10	.14	5.0	.13	4.0	.09	2.5	.15	4.0	.20	3.0
$\bar{x}$	.14		.17		.10		.15		.17	
s	.01		.04		.005		.02		.02	

Mean of $\bar{x}$'s = .15, Standard Deviation of $\bar{x}$'s = .03.

Copper Diaphragm, Inelastically Mounted, Impacts .32 Inch from Center.

Impact No.	Diaphragm Number 1		2		3		4		5	
	H	L	H	L	H	L	H	L	H	L
1	.08	5.0	.15	3.5	.11	5.0	.11	5.0	.11	4.0
2	.08	5.0	.12	3.5	.14	5.0	.10	5.0	.14	4.0
3	.10	5.0	.13	3.5	.07	5.0	.09	5.0	.10	4.0
4	.15	5.0	.10	3.5	.10	5.0	.11	5.0	.17	4.0
5	.15	5.0	.13	3.5	.08	5.0	.10	5.0	.15	4.0
6	.08	5.0	.10	3.5	.11	5.0	.09	5.0	.14	4.0
7	.10	5.0	.11	3.5	.06	5.0	.10	5.0	.12	4.0
8	.10	5.0	.12	3.5	.11	5.0	.11	5.0	.15	4.0
9	.14	5.0	.12	3.5	.14	5.0	.12	5.0	.13	4.0
10	.16	5.0	.10	3.5	.16	5.0	.07	5.0	.16	4.0
$\bar{x}$	.11		.12		.10		.10		.14	
s	.03		.02		.04		.01		.02	

Mean of $\bar{x}$'s = .11, Standard Deviation of $\bar{x}$'s = .02.

H indicates maximum pulse height in volts, L indicates pulse length in msec.

Appendix C (continued)

Polyethylene Diaphragm, Elastically Mounted, Impacts at Edge.

Impact No.	1 H	1 L	2 H	2 L	3 H	3 L	4 H	4 L	5 H	5 L
1	.8	1.0	1.2	1.0	1.1	1.0	1.5	1.0	.6	.5
2	1.0	1.0	1.7	1.0	.7	1.0	1.4	1.0	.6	.5
3	1.0	1.0	1.5	1.0	.7	1.0	1.6	1.0	.6	.5
4	.6	1.0	1.2	1.0	1.3	1.0	1.5	1.0	.5	.5
5	.5	1.0	1.2	1.0	1.6	1.0	1.5	1.0	.5	.5
6	1.0	1.0	1.5	1.0	1.4	1.0	1.3	1.0	.5	.5
7	.8	1.0	1.0	1.0	.8	1.0	1.7	1.0	.6	.5
8	1.3	1.0	1.7	1.0	1.4	1.0	1.5	1.0	.4	.5
9	1.0	1.0	1.0	1.0	.7	1.0	1.3	1.0	.5	.5
10	1.0	1.0	1.5	1.0	.6	1.0	1.2	1.0	.5	.5
$\bar{x}$	.90		1.35		1.03		1.45		.53	
s	.23		.26		.37		.15		.07	

Mean of $\bar{x}$'s = 1.05, Standard Deviation of $\bar{x}$'s = .37.

Polyethylene Diaphragm, Inelastically Mounted, Impacts at Edge.

Impact No.	1 H	1 L	2 H	2 L	3 H	3 L	4 H	4 L	5 H	5 L
1	.30	2.0	.30	2.0	.35	2.0	.25	2.0	.20	1.0
2	.30	2.0	.20	2.0	.25	2.0	.25	2.0	.15	1.0
3	.30	2.0	.20	2.0	.30	2.0	.30	2.0	.20	1.0
4	.30	2.0	.20	2.0	.35	2.0	.25	2.0	.20	1.0
5	.20	2.0	.20	2.0	.30	2.0	.30	2.0	.20	1.0
6	.25	2.0	.20	2.0	.40	2.0	.25	2.0	.20	1.0
7	.25	2.0	.15	2.0	.40	2.0	.20	2.0	.20	1.0
8	.25	2.0	.15	2.0	.35	2.0	.20	2.0	.20	1.0
9	.20	2.0	.20	2.0	.30	2.0	.25	2.0	.20	1.0
10	.25	2.0	.20	2.0	.35	2.0	.20	2.0	.20	1.0
$\bar{x}$	.26		.20		.34		.25		.20	
s	.04		.04		.05		.04		.02	

Mean of $\bar{x}$'s = .25, Standard Deviation of $\bar{x}$'s = .06.

H indicates maximum pulse height in volts, L indicates pulse length in msec.

Appendix C (continued)

Aluminum Diaphragm, Elastically Mounted, Impacts at Edge.

Impact No.	1 H	1 L	2 H	2 L	3 H	3 L	4 H	4 L	5 H	5 L
1	.6	.5	.6	.5	.8	.5	.3	.5	.4	1.0
2	.7	.5	.5	.5	.4	.5	.2	.5	.3	1.0
3	.6	.5	.6	.5	.7	.5	.2	.5	.3	1.0
4	.8	.5	.5	.5	.5	.5	.3	.5	.2	1.0
5	.8	.5	.5	.5	.4	.5	.2	.5	.3	1.0
6	.6	.5	.5	.5	.4	.5	.2	.5	.3	1.0
7	.5	.5	.5	.5	.6	.5	.3	.5	.4	1.0
8	.8	.5	.6	.5	.7	.5	.3	.5	.3	1.0
9	.6	.5	.4	.5	.7	.5	.2	.5	.3	1.0
10	.6	.5	.5	.5	.6	.5	.3	.5	.3	1.0
$\bar{x}$	.60		.52		.58		.25		.31	
s	.09		.06		.15		.05		.06	

Mean of $\bar{x}$'s = .45, Standard Deviation of $\bar{x}$'s = .16.

Aluminum Diaphragm, Inelastically Mounted, Impacts at Edge.

Impact No.	1 H	1 L	2 H	2 L	3 H	3 L	4 H	4 L	5 H	5 L
1	.02	6.0	1.0	1.0	.04	5.0	.03	5.0	.03	3.0
2	.03	6.0	1.0	1.0	.03	5.0	.03	5.0	.03	3.0
3	.03	6.0	1.3	1.0	.04	5.0	.03	5.0	.03	3.0
4	.03	6.0	1.3	1.0	.03	5.0	.03	5.0	.03	3.0
5	.04	6.0	1.2	1.0	.03	5.0	.03	5.0	.03	3.0
6	.03	6.0	1.4	1.0	.04	5.0	.03	5.0	.03	3.0
7	.03	6.0	1.3	1.0	.03	5.0	.03	5.0	.03	3.0
8	.02	6.0	.9	1.0	.03	5.0	.03	5.0	.03	3.0
9	.02	6.0	1.2	1.0	.03	5.0	.02	5.0	.03	3.0
10	.02	6.0	1.4	1.0	.04	5.0	.03	5.0	.03	3.0
$\bar{x}$	.02		1.20		.03		.03		.03	
s	.01		.18		.01		.00		.00	

Mean of $\bar{x}$'s = .26, Standard of $\bar{x}$'s = .52.

H indicates maximum pulse height in volts, L indicates pulse length in msec.

Appendix C (continued)

Steel Diaphragm, Elastically Mounted, Impacts at Edge.

Impact No.	Diaphragm Number									
	1		2		3		4		5	
	H	L	H	L	H	L	H	L	H	L
1	.06	1.5	.08	1.5	.15	2.0	1.5	1.5	1.5	1.5
2	.04	1.5	.08	1.5	.20	2.0	1.5	1.5	1.5	1.5
3	.08	1.5	.08	1.5	.20	2.0	1.5	1.5	1.5	1.5
4	.05	1.5	.08	1.5	.15	2.0	1.5	1.5	1.6	1.5
5	.08	1.5	.10	1.5	.20	2.0	1.5	1.5	1.5	1.5
6	.07	1.5	.10	1.5	.20	2.0	1.5	1.5	1.5	1.5
7	.08	1.5	.10	1.5	.20	2.0	1.6	1.5	1.5	1.5
8	.08	1.5	.10	1.5	.20	2.0	1.5	1.5	1.8	1.5
9	.08	1.5	.10	1.5	.20	2.0	1.4	1.5	1.5	1.5
10	.08	1.5	.10	1.5	.20	2.0	1.5	1.5	1.8	1.5
$\bar{x}$	.07		.09		.19		1.50		1.57	
s	.01		.01		.02		.05		.13	

Mean of $\bar{x}$'s = .68, Standard Deviation of $\bar{x}$'s = .78.

Steel Diaphragm, Inelastically Mounted, Impacts at Edge.

Impact No.	Diaphragm Number									
	1		2		3		4		5	
	H	L	H	L	H	L	H	L	H	L
1	.05	1.5	.08	2.5	.06	1.5	.4	1.5	.04	2.0
2	.08	1.5	.08	2.5	.05	1.5	.6	1.5	.06	2.0
3	.05	1.5	.08	2.5	.04	1.5	.8	1.5	.05	2.0
4	.06	1.5	.08	2.5	.06	1.5	.6	1.5	.07	2.0
5	.05	1.5	.08	2.5	.06	1.5	.7	1.5	.05	2.0
6	.07	1.5	.08	2.5	.05	1.5	.6	1.5	.08	2.0
7	.06	1.5	.08	2.5	.05	1.5	.7	1.5	.08	2.0
8	.07	1.5	.08	2.5	.05	1.5	.8	1.5	.08	2.0
9	.08	1.5	.08	2.5	.06	1.5	.7	1.5	.08	2.0
10	.04	1.5	.08	2.5	.06	1.5	.7	1.5	.08	2.0
$\bar{x}$	.06		.08		.05		.66		.08	
s	.02		.00		.01		.12		.02	

Mean of $\bar{x}$'s = .19, Standard Deviation of $\bar{x}$'s = .27.

H indicates maximum pulse height in volts, L indicates pulse length in msec.

Appendix C (continued)

Copper Diaphragm, Elastically Mounted, Impacts at Edge.

Impact No.	Diaphragm Number 1		2		3		4		5	
	H	L	H	L	H	L	H	L	H	L
1	.35	3.0	.30	2.0	.35	3.0	.30	2.0	.20	2.0
2	.40	3.0	.25	2.0	.30	3.0	.30	2.0	.35	2.0
3	.25	3.0	.25	2.0	.30	3.0	.30	2.0	.30	2.0
4	.35	3.0	.25	2.0	.30	3.0	.25	2.0	.30	2.0
5	.40	3.0	.30	2.0	.30	3.0	.25	2.0	.30	2.0
6	.30	3.0	.25	2.0	.30	3.0	.30	2.0	.30	2.0
7	.40	3.0	.20	2.0	.35	3.0	.30	2.0	.30	2.0
8	.35	3.0	.20	2.0	.40	3.0	.25	2.0	.25	2.0
9	.35	3.0	.30	2.0	.30	3.0	.25	2.0	.30	2.0
10	.40	3.0	.20	2.0	.25	3.0	.30	2.0	.30	2.0
$\bar{x}$	.36		.25		.32		.28		.29	
s	.05		.04		.04		.03		.04	

Mean of $\bar{x}$'s = .30, Standard Deviation of $\bar{x}$'s = .04.

Copper Diaphragm, Inelastically Mounted, Impacts at Edge.

Impact No.	Diaphragm Number 1		2		3		4		5	
	H	L	H	L	H	L	H	L	H	L
1	.08	6.0	.04	6.0	.04	5.0	.06	5.0	.06	5.0
2	.08	6.0	.06	6.0	.06	5.0	.05	5.0	.06	5.0
3	.08	6.0	.05	6.0	.06	5.0	.06	5.0	.06	5.0
4	.08	6.0	.07	6.0	.05	5.0	.05	5.0	.07	5.0
5	.08	6.0	.05	6.0	.08	5.0	.05	5.0	.07	5.0
6	.08	6.0	.07	6.0	.07	5.0	.05	5.0	.06	5.0
7	.08	6.0	.06	6.0	.06	5.0	.05	5.0	.07	5.0
8	.07	6.0	.06	6.0	.07	5.0	.04	5.0	.05	5.0
9	.08	6.0	.07	6.0	.07	5.0	.05	5.0	.07	5.0
10	.08	6.0	.07	6.0	.06	5.0	.06	5.0	.07	5.0
$\bar{x}$	.08		.06		.06		.05		.06	
s	.00		.01		.01		.01		.01	

Mean of $\bar{x}$'s = .06, Standard Deviation of $\bar{x}$'s = .01.

H indicates maximum pulse height in volts, L indicates pulse length in msec.

Appendix D

Flow Rate Test

Run No.	Sample Time (minutes)	Experimental Count	Counts per Minute	Actual Count	Counts per Minute
1	.50	9393	18786	15041	30082
2	.50	10656	21312	24550	49100
3	.50	10458	20916	22410	44820
4	.50	9470	18940	18401	36082
5	.50	7044	14088	10760	21520
6	.50	6843	13686	10147	20294
7	.50	5873	11746	8103	16206
8	.50	4946	9892	6413	12826
9	.50	3136	6272	3956	7912
10	.50	2151	4302	2712	5424
11	1.00	2880	2880	3723	3723
12	1.00	2070	2070	2435	2435
13	1.00	1204	1204	1614	1614
14	1.00	726	726	858	858

Pulse Length, 2.0 msec. Trigger Level, .10 volt.

1	1.00	2736	2736	3601	3601
2	1.00	7049	7049	8768	8768
3	1.00	10184	10184	13188	13188
4	1.00	8475	8475	10622	10622
5	1.00	10098	10098	13222	13222
6	1.00	DATA	REJECTED		
7	.50	8745	17490	16862	33724
8	1.00	8565	8565	10981	10981
9	1.00	10892	10892	14321	14321
10	1.00	13993	13993	19982	19982
11	1.00	7902	7902	9601	9601
12	1.00	9664	9664	12049	12049
13	1.00	5585	5585	6941	6941
14	1.00	3793	3793	4762	4762
15	1.00	1721	1721	2260	2260
16	.25	3808	15232	5140	20560
17	.25	4607	18428	6746	26948
18	.25	5351	21404	9674	38696
19	.25	6092	24368	13162	52648
20	.25	6345	25380	14818	59272

Pulse Length, 1.5 msec. Trigger Level, .10 volt.

COMBINE GRAIN LOSS TRANSDUCER DESIGN

by

JAMES DOMENIC SCHARPLAZ

B. S., Kansas State University, 1973

AN ABSTRACT OF A MASTER'S THESIS

submitted in partial fulfillment of the

requirements for the degree

MASTER OF SCIENCE

Department of Agricultural Engineering

KANSAS STATE UNIVERSITY
Manhattan, Kansas

1975

ABSTRACT

The purpose of this thesis was to design a transducer that could monitor combine grain loss. Cylinder or unthreshed grain loss was of particular interest. Based on findings by Zaidi, it was decided to predict cylinder loss by measuring the ratio of the amount of grain threshed at two different positions on the combine concave.

First an attempt was made to measure the amount of grain threshed by weighing it continuously with a cantelever beam device. Calculations showed the device would be susceptible to machine vibration, so it was dropped. Attention was then directed to counting the kernels individually as they struck a diaphragm.

Design of the impact counting transducer proceeded in two steps. First, various diaphragm materials were tested by dropping individual lead shot on the transducer. Polyethylene was selected as the material producing the best combination of amplitude, short pulse length, and least pulse attenuation as the impacts moved from the center of the transducer. The second step involved subjecting the counter to various flow rates of wheat. The kernels were caught as they bounced off the diaphragm and were then recounted to determine the actual flow rate. The results were plotted and equations developed to predict actual rate from the transducer output.

The counter was capable of counting at approximately five times the design rate, and was insensitive to vibration when equipped with the right transducer. It was sealed to prevent damage by dust and moisture, and was small enough not to obstruct operation of the machine.